CHAPTER 3

FORCES ON WALLS

Section I. Introduction

3-1. General. Retaining walls and flood walls accommodate a difference in soil or water elevation over a typically short horizontal distance. On one side of the wall, the driving side, lateral forces exceed those on the opposite, resisting side; the force difference and resulting moment are accommodated by forces and pressures developed along the base. Lateral forces may be related to gravity, water seepage, waves, wind, and earthquakes. This chapter presents methods for calculating pressures and resulting forces on the driving and resisting sides of walls. These are necessary to calculate the magnitude and location of the base resultant force for overturning and bearing capacity analysis. They are also required for the design of the structural elements of the wall.

3-2. Limit-Equilibrium Analysis. The forces and pressures acting on a wall are in fact highly indeterminate. Static equilibrium equations are insufficient to obtain a solution for lateral forces; additional assumptions must be incorporated in the analysis. For nonlinear materials such as soils, this is commonly and conveniently done by assuming that a "limit" or failure state exists along some surface and that the shear force along the surface corresponds to the shear strength of the material. With these assumptions, equilibrium equations can be solved. Hence, this approach is commonly called "limit-equilibrium analysis." To assure that the assumed failure does not in fact occur, a factor (safety factor or strength mobilization factor) is applied to the material strength. It should be noted that this solution approach differs significantly from that commonly used for indeterminate structural analysis, where stress-strain properties and deformations are employed. This limit-equilibrium approach provides no direct information regarding deformations; it is implied that deformations are sufficient to induce the failure condition. Deformations are indirectly limited to tolerable values by judicious choice of a safety factor.

3-3. Relationship of Forces to Sliding Analysis. Forces calculated in accordance with this chapter are not always equal to those calculated in a sliding analysis (Chapter 4). The methods in this chapter are intended to produce reasonable and somewhat conservative estimates of actual forces operative on the wall. They can be used to perform a quick check on sliding stability as described in paragraph 4-15. The sliding analysis for general cases (paragraph 4-16) considers shear failure along the bases of a collection of interacting free bodies (or wedges) that include both the wall and surrounding soil. Sliding failure is prevented by applying a factor of safety on shear strength equally on all segments of the failure surface. The lateral forces calculated in the sliding analysis are a function of the sliding factor of safety.

Section II. Earth Pressures and Forces

3-4. Cohesionless Materials.

a. Active Earth Pressure. Cohesionless materials such as clean sand are the recommended backfill for retaining walls. Large-scale tests (e.g., Terzaghi 1934; Tschebatarioff 1949; Matsuo, Kenmochi, and Yagi 1978) with cohesionless (c = 0) backfills have shown that horizontal pressures are highly dependent on the magnitude and direction of wall movement. The minimum horizontal pressure condition, or active earth pressure, develops when a wall rotates about its base and away from the backfill an amount on the order of 0.001 to 0.003 radian (a top deflection of 0.001 to 0.003h , where h is the wall height). As the wall moves, horizontal stresses in the soil are reduced and vertical stresses due to backfill weight are carried by increasing shear stresses until shear failure is imminent (see Figure 3-1a).

b. Passive Earth Pressure. If a wall is moved toward the backfill, horizontal stresses increase and shear stresses reverse direction, first decreasing and then increasing to a maximum at failure (see Figure 3-1b). Because the horizontal stress component along the shear planes is resisted by both shear stress and vertical stress components, higher horizontal stresses can be developed than for the active pressure case. Development of the maximum possible horizontal stress, or passive pressure, requires much larger wall rotations than for the active case, as much as 0.02 to 0.2 radian. It should be noted that the deformation required to mobilize one-half of the passive pressure is significantly smaller than that required for full mobilization.

c. At-Rest Earth Pressure. If no wall movement occurs, the lateral pressure condition is termed the at-rest pressure.

d. Lateral Earth Pressure Coefficient K. The ratio of the horizontal effective stress to the vertical effective stress in a cohesionless soil mass can be expressed by the earth pressure coefficient K . Typical relationships between the K value and wall movements are shown in Figure 3-2. The value of K can be obtained for active (K_A) and passive (K_P) conditions using limit-equilibrium methods. Empirical equations are available for the at-rest value (K_o) as described in paragraph 3-10.

e. Conditions Affecting Earth Pressure. For complicated backfill conditions, at-rest earth forces can be estimated using the general wedge method combined with factored soil strengths as described in paragraph 3-13. If the mode of wall movement is other than base rotation, the earth pressure and its distribution may differ considerably from any solutions herein and other analysis techniques are required (see paragraph 3-15g). Also, compaction of the backfill behind a wall can produce horizontal pressures in excess of at-rest pressures near the top of a wall as discussed in paragraph 3-17.

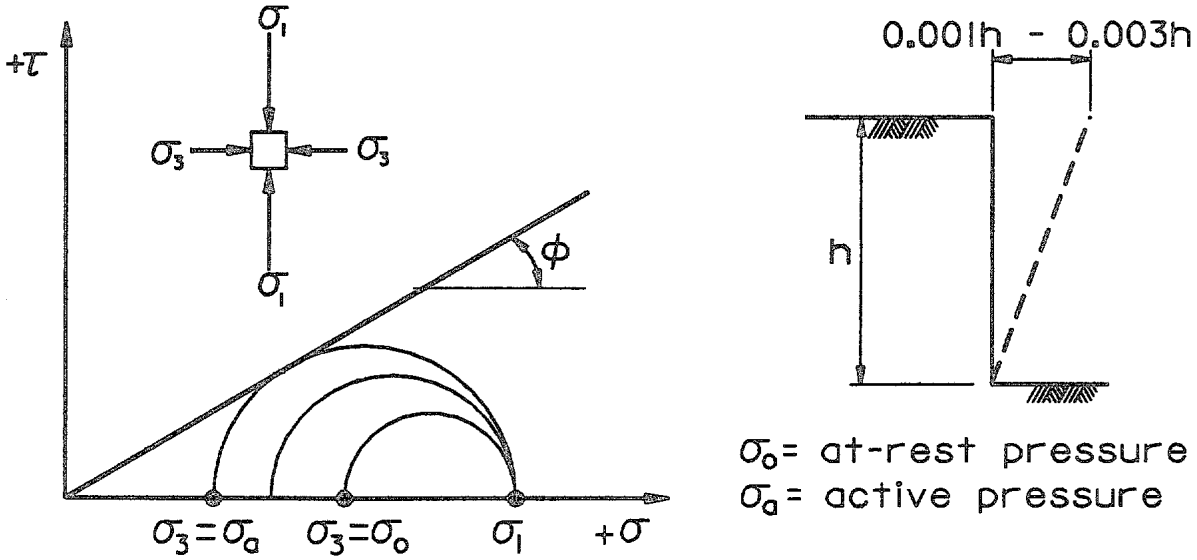

a. Development of active earth pressure

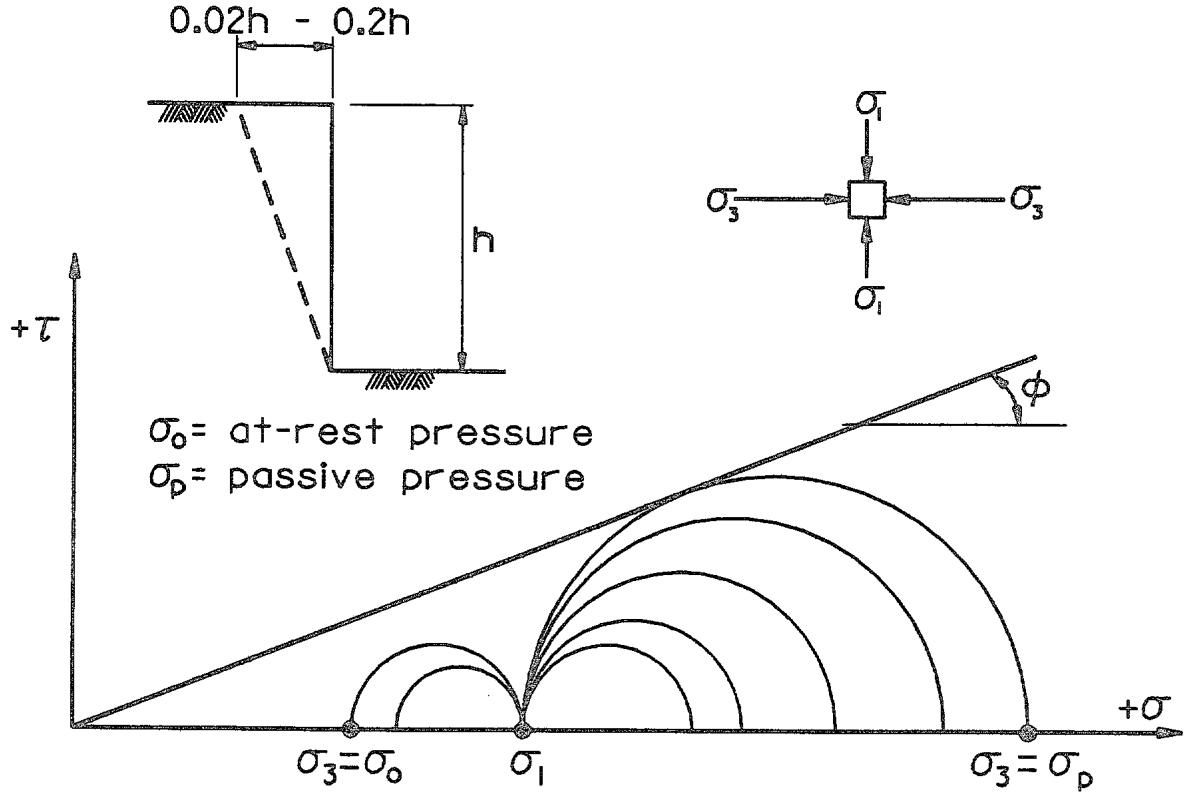

b. Development of passive earth pressure

Figure 3-1. Development of earth pressures for a cohesionless material

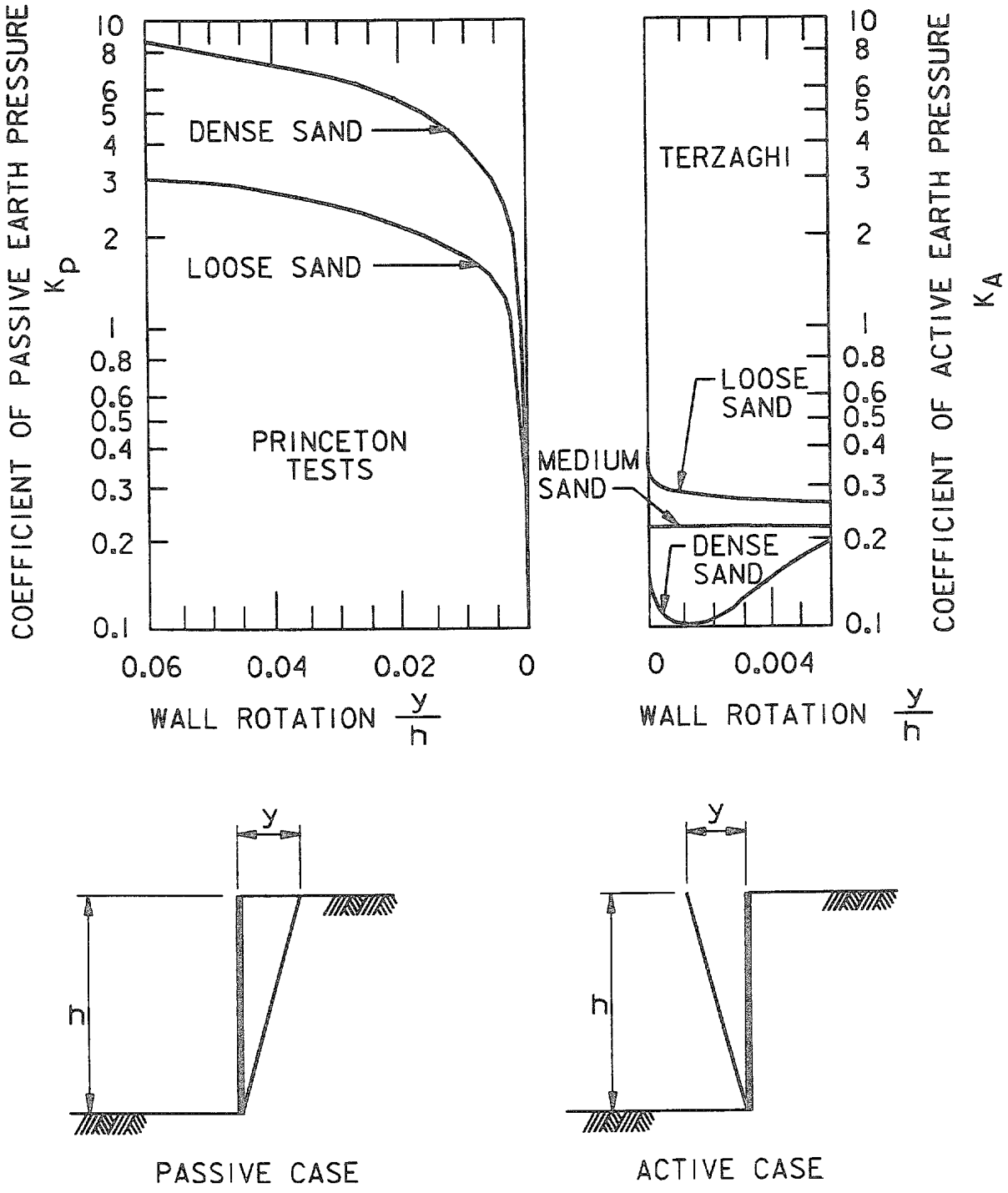

Figure 3-2. Relationship of earth pressures to wall movements (after Department of the Navy 1982b)

3-5. Cohesive Materials.

a. Strength Properties. So-called cohesive materials, typically fine-grained soils such as clay, exhibit shear strength under zero confining stress when loaded rapidly. The strength at zero confinement is expressed by the parameter c, or cohesion. Cohesive materials are usually saturated or nearly saturated because their small pore diameter attracts capillary water. When stress changes are imposed (such as by wall movement) the soil attempts to change volume. If low permeability prevents volume change from keeping pace with the external stress change, pressure changes are induced in the pore water. What appears to be stress-independent strength (cohesion) is, for the most part, the combined effects of frictional resistance between soil particles and induced pore pressure changes. Pore water tension at low stresses permits vertical cuts in clay; however, such cuts eventually fail as negative pore pressures dissipate and water content increases. Horizontal pressures in cohesive materials are related to the soil's permeability and pore pressure response during shear in addition to wall movement. Therefore they are time dependent.

b. Use as a Backfill Material. It is strongly recommended that cohesionless materials such as clean sands be used for wall backfill materials. Cohesionless materials have more predictable properties than cohesive materials, are less frost susceptible, and provide better drainage. However, there are certain instances (such as walls adjacent to impervious clay cutoffs in flood-control structures) where clay backfills may be unavoidable.

c. Short- and Long-Term Analyses. Solutions are included herein for earth pressures in the terms of the general case involving both the c and ϕ parameters. Where cohesive backfills are used, two analyses (short-term and long-term) are usually required with different sets of strength parameters in order to model conditions that may arise during the life of the wall. Strength tests are further discussed in Chapter 2, Section V.

(1) Short-Term Analyses. These analyses model conditions prevailing before pore pressure dissipation occurs, such as the end-of-construction condition. For these analyses, unconsolidated-undrained (Q) test parameters are appropriate. Often these tests yield a relatively high c value and a low or zero ϕ value. Calculations may indicate that the soil is in tension to significant depths and exerts zero pressure on the wall; thus, the short-term analysis alone will seldom govern wall design. However, the zone of theoretically negative soil pressure may correspond to cracking and should be assumed to crack as described in paragraphs 3-15f and 4-18. Water entering these cracks may exert significant horizontal pressure on a wall. Therefore, short-term stability analyses should include a check of the effect of water pressure in tension cracks.

(2) Long-Term Analyses. These analyses model conditions prevailing after shear-induced excess pore pressures have dissipated. (Dissipation herein includes negative pore pressures increasing to zero.) For long-term analysis, consolidated-drained (S) test parameters are appropriate. These

tests usually yield a relatively high ϕ value and a relatively low or zero c value.

d. Overconsolidated "Swelling" Clay Soils. For highly overconsolidated and/or "swelling" clay soils, lateral pressures may be developed in excess of those calculated using drained or undrained strength parameters. These pressures cannot generally be determined using limit-equilibrium techniques (see, e.g., Brooker and Ireland 1965). The use of such soils around retaining walls should be avoided.

3-6. Pressures in Soil-Water Systems. Soil grains are able to transmit shear stresses; water cannot. Consequently, effective pressures in soil may differ on horizontal and vertical planes but water pressures cannot. Effective soil pressures are therefore separated from water pressures in calculations. If the value of K is established, horizontal effective stresses may be calculated by multiplying the effective vertical stress at any point by the corresponding K value (see Figure 3-3). To obtain the total horizontal pressure, the effective horizontal pressure is added to the water pressure. Where more than one soil layer is present, vertical pressures increase continuously with depth but the horizontal pressure diagrams may be discontinuous as shown. Combining water pressures with effective earth pressures is further discussed in paragraphs 3-15 and 3-18.

3-7. Design Earth Pressures and Forces, Driving Side.

a. Use of At-Rest Earth Pressures. The driving side of a retaining wall or flood wall is defined as that side on which soil and/or water exerts a horizontal force tending to cause instability. Designers have often assumed active earth pressure on the driving side because movements required to develop active pressures are small. However, several reasons exist to design walls for at-rest pressures. Because designs incorporate factors of safety, walls may be quite rigid and pressures may be greater than active. Hydraulic structures in particular are designed using conservative criteria that result in relatively stiff wall designs. Walls founded on rock or stiff soil foundations may not yield sufficiently to develop active earth pressures. Even for foundations capable of yielding, certain experiments with granular backfill (Matsuo, Kenmochi, and Yagi 1978) indicate that, following initial yield and development of active pressures, horizontal pressures may in time return to at-rest values. Another reference (Casagrande 1973) states that the gradual buildup of the backfill in compacted lifts produces greater-than-active pressures as do long-term effects from vibrations, water level fluctuations, and temperature changes.

b. Estimation of Operative Pressures. Design analyses require an estimate of the expected "operative" (nonfailure) pressures on the wall for overturning and bearing capacity analyses and structural design. Therefore, walls should be designed to be safe against overturning and bearing failure for at-rest earth pressure conditions, and structural elements should be designed assuming at-rest earth pressures on the driving side. The lateral soil forces calculated using the multiple wedge sliding analysis described in Chapter 4

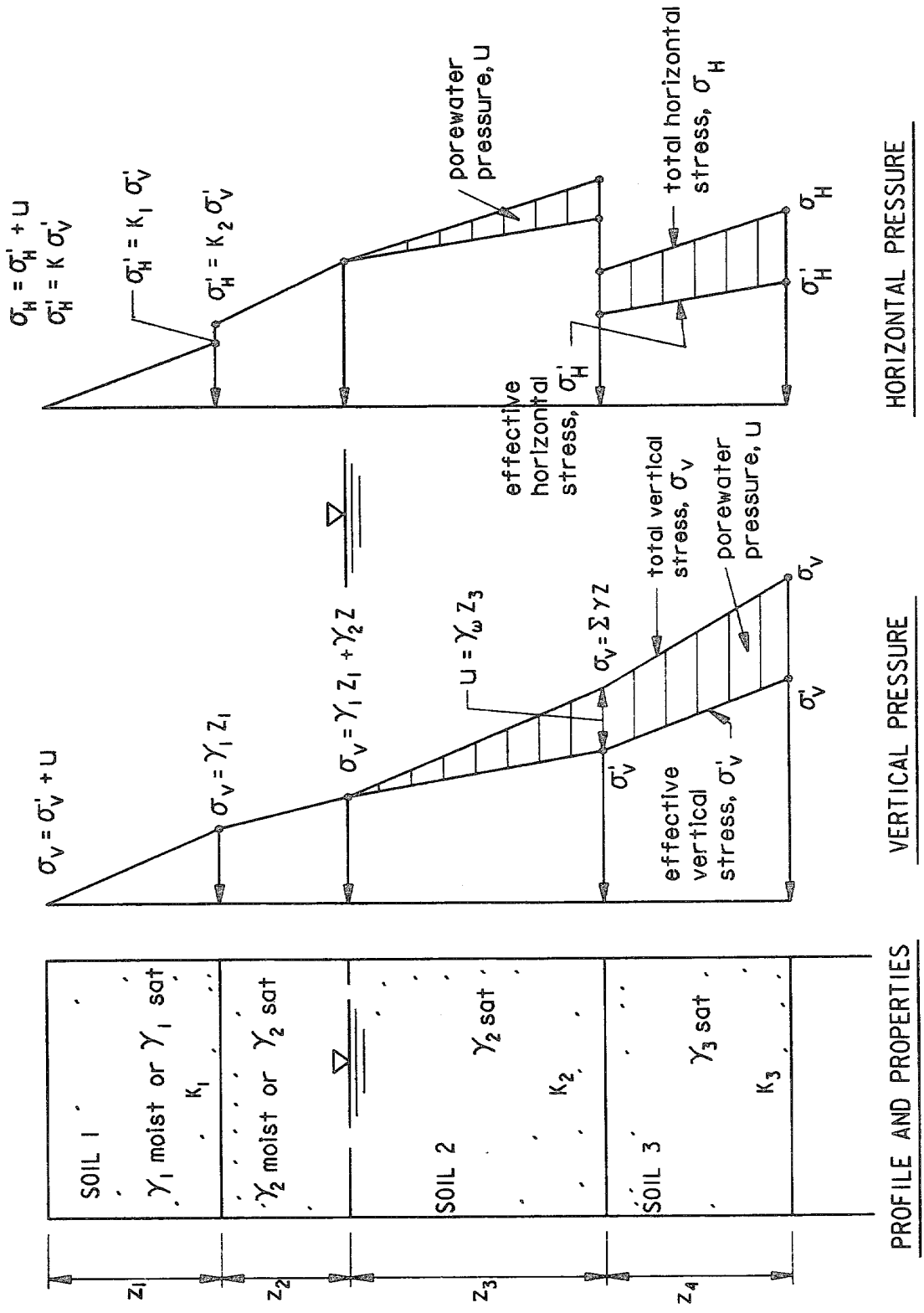

Figure 3-3. Vertical and horizontal pressures in a cohesionless soil mass

are in the at-rest pressure range when a safety factor of 1.5 is obtained.

c. Compaction and Surcharge Effects. Where significant compaction effort is specified for the backfill, design earth pressures should be increased beyond the at-rest values for depths above a "critical" depth as described in paragraph 3-17. Where surcharges are expected above the backfill (in stockpiles, rails, footings, etc.), the additional horizontal earth pressure due to the surcharge should be determined as discussed in paragraph 3-16 and superimposed on the at-rest pressure diagram. Examples of these effects are given in Appendix M.

3-8. Design Earth Pressures and Forces, Resisting Side.

a. Background. The resisting side of a wall is defined as that side where soil and/or water provide a lateral reaction tending to resist instability. The maximum earth force that can be developed is the passive earth force. However, for a wall in equilibrium, the actual resisting-side force will typically be smaller than the passive force as the forces on the driving side, base, and resisting side taken together must satisfy static equilibrium. The resistances to the driving-side force provided by the resisting-side force and the base shear force, respectively, are indeterminate. Allocation of the total resistance between these two forces is judgmental.

b. Estimation of Passive Resistance. A conservative and convenient design approach is to assume the resisting-side force is zero for overturning and bearing capacity analyses and for structural design. However, in some cases, such as walls with relatively deep foundations, it may be desirable to consider some lateral resistance for these analyses. To justifiably assume a non-zero resisting-side force, the material must not lose its resistance characteristics with any probable change in water content or environmental conditions and must not be eroded or excavated during the life of the wall. If such assumptions can be justified, at-rest conditions may be conservatively assumed on the resisting side. Resisting-side pressures and forces generally should not be assumed to exceed at-rest conditions when calculating the base resultant force and location and when designing structural components. However, if the driving-side earth force exceeds the sum of the resisting side at-rest earth force (if present) and the maximum available base shear force calculated using unfactored shear parameters, the additional required resistance should be assumed to be provided by additional resisting-side pressure. In no case should the resisting-side earth pressure exceed one-half the passive pressure calculated using unfactored shear strengths for overturning and bearing capacity analyses and structural design.

c. Horizontal Force Allocation. To summarize, the horizontal force allocation for overturning analysis, bearing capacity analysis, and design of structural components should be computed as follows:

(1) Calculate the at-rest effective earth force on the driving side (paragraphs 3-10 through 3-13). Superimpose surcharge effects if present (paragraph 3-16). Add water pressures, if present.

(2) Assume that the resisting-side earth force equals zero or calculate and apply the at-rest earth force on the resisting side of the wall, if justified (paragraphs 3-10 through 3-13). Add water forces if present.

(3) Assume that the horizontal component of the base resultant is equal to the difference between the horizontal forces from (1) and (2).

(4) If the maximum available base shear force is exceeded, assume that the remaining horizontal force is resisted by mobilizing a greater fraction of passive pressure so long as not more than one-half the available passive force is used. (This may occur where the resisting-side soil is strong relative to the driving-side and base soils.)

d. Sliding Stability Check. Sliding stability should be checked using the single or multiple wedge methods found in paragraphs 4-15 and 4-16, respectively.

3-9. Design Earth Pressures and Forces on the Base.

a. Calculation of Resultant Force on Base. The resultant force on the base, its direction, and its location must be such that the wall is in static equilibrium for the "operative" loads (see Figure 3-4). In Figure 3-4a, the vertical component of the resultant is equal and opposite the summed weights of the "structural wedge" and the horizontal component is equal to the difference of the driving-side and resisting-side forces. Figure 3-4b illustrates a more complicated example including water and a sloping base with a key. The vertical and horizontal components of the base uplift force are calculated from base water pressures obtained from a seepage analysis. The remaining vertical and horizontal forces required for equilibrium are provided by components of the base shear force T and effective normal force N'. An overturning analysis as described in Chapter 4 must be performed in order to determine the effective normal force N' and its location.

b. Computation of Base Pressures. The effective earth pressure on the base is assumed to vary linearly and N' is applied at the centroid of the pressure diagram. When the resultant falls within the middle one-third of the base, the effective base pressures q' are calculated by the following equation:

$$q' = \left(\frac{N'}{B}\right)\left(1 \pm \frac{6e}{B}\right) \qquad [3\text{-}1]$$

where

N' = effective normal force on base of structure

B = width of base of structure

e = eccentricity of N' from center of base

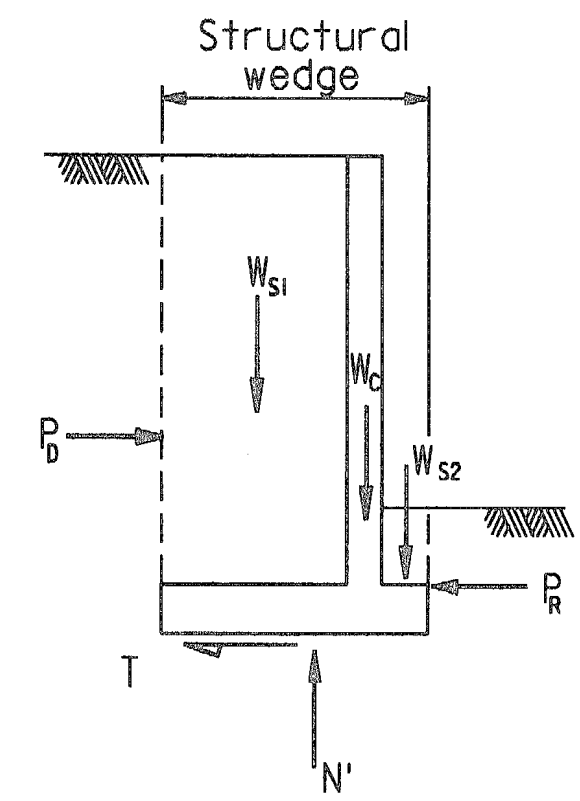

$N' = \Sigma W$

$T = P_D - P_R$

a. Simple retaining wall

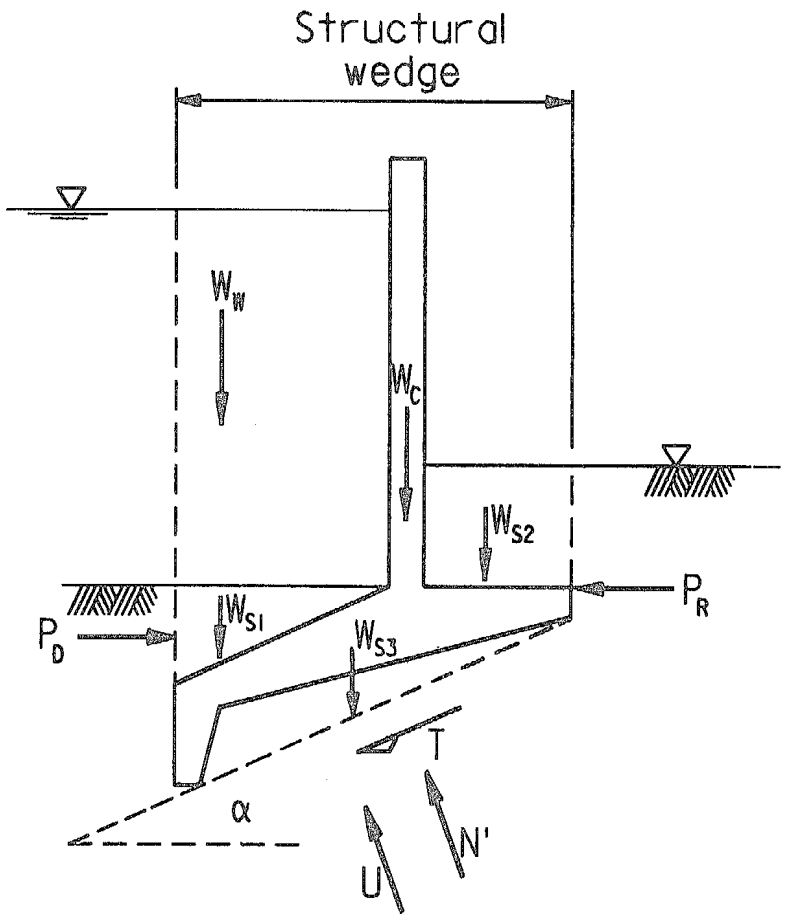

$T = \Sigma H \cos\alpha - \Sigma V \sin\alpha$ $\qquad N' = \Sigma V \cos\alpha + \Sigma H \sin\alpha$

ΣH and ΣV are summation of all forces not including T and N'

b. Flood wall with sloping base and key

Figure 3-4. Forces on base of wall

This is shown in Figure 3-5, a and b. If the resultant falls outside the middle one-third of the base, i.e., e is greater than B/6 , as shown in Figure 3-5c, the pressure distribution is triangular with a maximum pressure equal to

$$q'_{max} = \frac{4}{3}\left(\frac{N'}{B - 2e}\right) \qquad [3-2]$$

The base will be in compression over a distance b from the toe computed as

$$b = \frac{3}{2}(B - 2e) \qquad [3-3]$$

Refer to Appendix N for example computations.

3-10. At-Rest Earth Pressure Equations.

a. Horizontal Backfill. For the special case of a horizontal backfill surface and a normally consolidated backfill (no compaction or other prestress effects) the at-rest pressure coefficient K_o can be estimated from Jaky's (1944) equation

$$K_o = 1 - \sin \phi' \qquad [3-4]$$

and the lateral earth pressure computed by

$$p_o = \gamma' K_o z$$

where

ϕ' = drained internal friction angle

γ' = effective unit weight (moist or saturated above water table, submerged or buoyant below water table)

z = depth below surface of backfill along a vertical plane

b. Sloping Backfills. For normally consolidated sloping backfills, results of experiments to measure K_o are quite variable. The following equation proposed by the Danish Code (Danish Geotechnical Institute 1978) is recommended:

$$K_{o\beta} = K_o (1 + \sin \beta) \qquad [3-5]$$

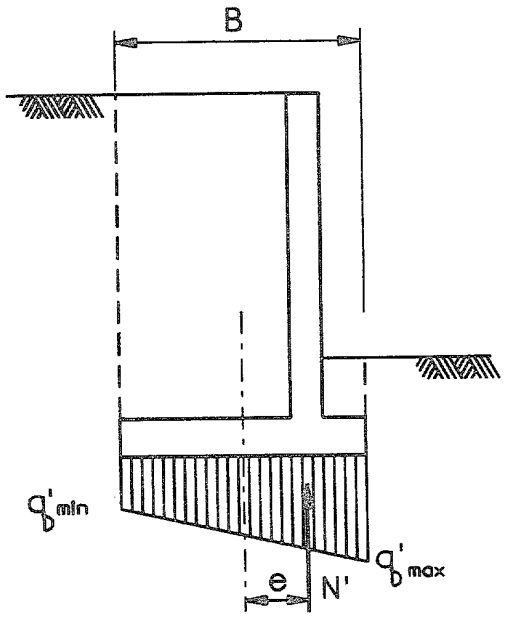

$$q'_b = \frac{N'}{A} \pm \frac{Mc}{I}$$

$$q'_{b\,max} = \left(\frac{N'}{B}\right)\left(1 + \frac{6e}{B}\right)$$

$$q'_{b\,min} = \left(\frac{N'}{B}\right)\left(1 - \frac{6e}{B}\right)$$

a. Simple wall, resultant in middle one-third of base

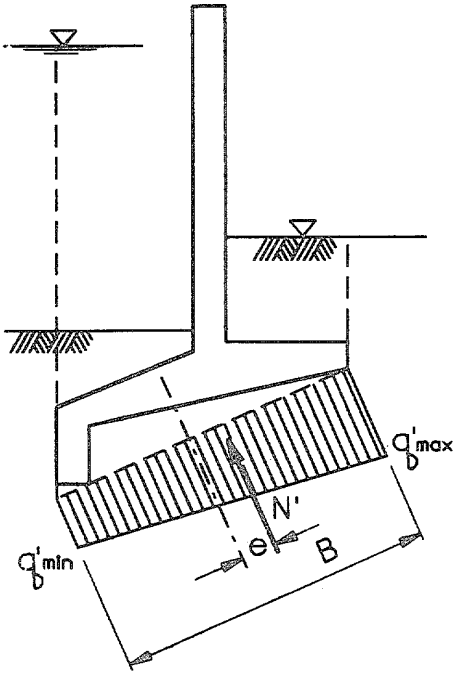

b. Flood wall with sloping base

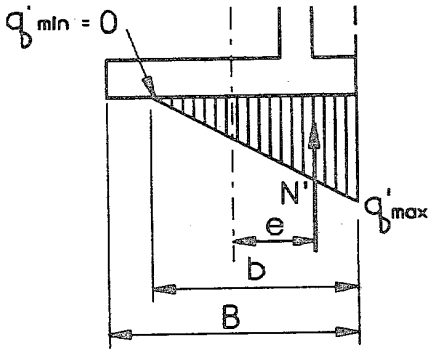

$$q'_{b\,max} = \left(\frac{4}{3}\right)\left(\frac{N'}{B - 2e}\right)$$

$$b = \left(\frac{3}{2}\right)(B - 2e)$$

c. Pressure for resultant outside middle one-third

Figure 3-5. Base pressures

Substituting Equation 3-4 in 3-5 gives:

$$K_{o\beta} = (1 - \sin \phi')\ (1 + \sin \beta) \qquad [3\text{-}6]$$

and the lateral earth pressure computed by

$$p_o = \gamma' K_{o\beta} z$$

where β is the slope angle from the horizontal. β is positive for a soil layer that slopes upward and away from the structure. Values for K_o and $K_{o\beta}$ are given in Appendix E.

c. General Conditions. For walls with irregular backfill surfaces, non-homogeneous backfills, surcharge loadings, and/or other complicating conditions, empirical relationships for the at-rest pressure are not generally available. For routine designs, an approximate solution for the horizontal earth force may be obtained using Coulomb's active force equation or the general wedge method with values of c and $\tan \phi$ multiplied by a strength mobilization factor (defined in paragraph 3-11). Because this is an empirical approach, results will differ slightly from calculations using Equations 3-4 through 3-6 where companion solutions can be obtained. Appendix E includes a comparison of K_o values so obtained for both horizontal and sloping backfills. Figure 3-6 shows a comparison of Jaky's equation with Coulomb's equation for a horizontal backfill.

d. Resisting Side. Jaky's equation and the Danish Code equation may be used to compute at-rest pressures for the resisting side for horizontal and sloping soil surfaces, respectively. Example computations are shown in example 7 of Appendix M and in Appendix N.

3-11. Strength Mobilization Factor.

a. Definition. The strength mobilization factor (SMF) is defined as the ratio of the assumed mobilized or developed shear stress τ along an assumed slip surface to the maximum shear strength τ_f of the soil material at failure. If an appropriate SMF value is assumed and applied to c and $\tan \phi$, it allows calculation of greater-than-active earth pressures using Coulomb's active force equation (paragraph 3-12) or the general wedge equation (paragraph 3-13). Alternatively, the safety against sliding may be assessed by calculating the average SMF along an assumed sliding surface from an equilibrium analysis and comparing it to a recommended maximum value. These concepts are illustrated in Figure 3-7. In equation form, the strength mobilization factor may be expressed as:

$$SMF = \frac{\tau}{\tau_f} \qquad [3\text{-}7]$$

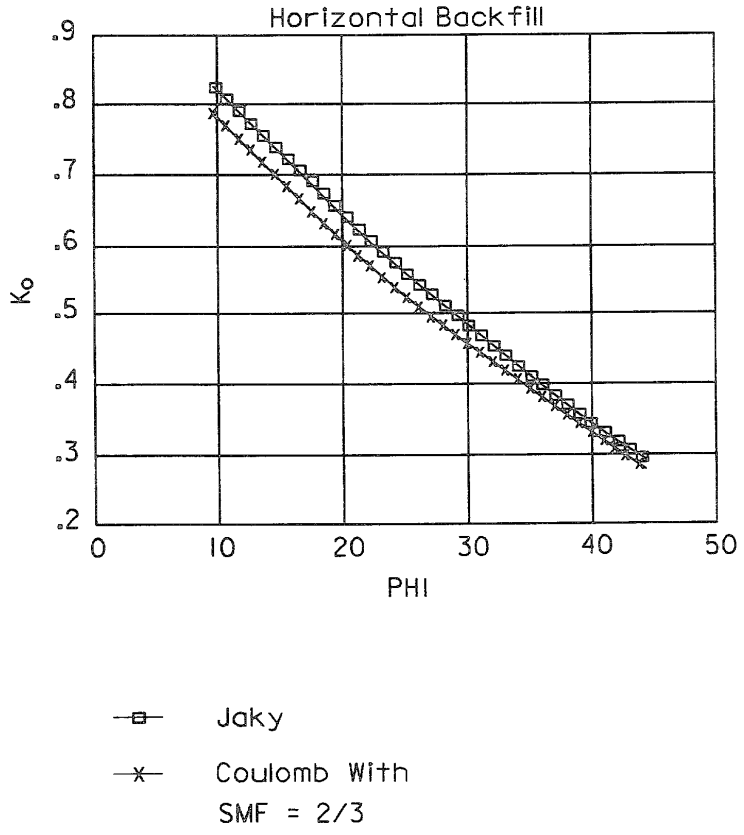

Figure 3-6. At-rest earth pressure coefficients

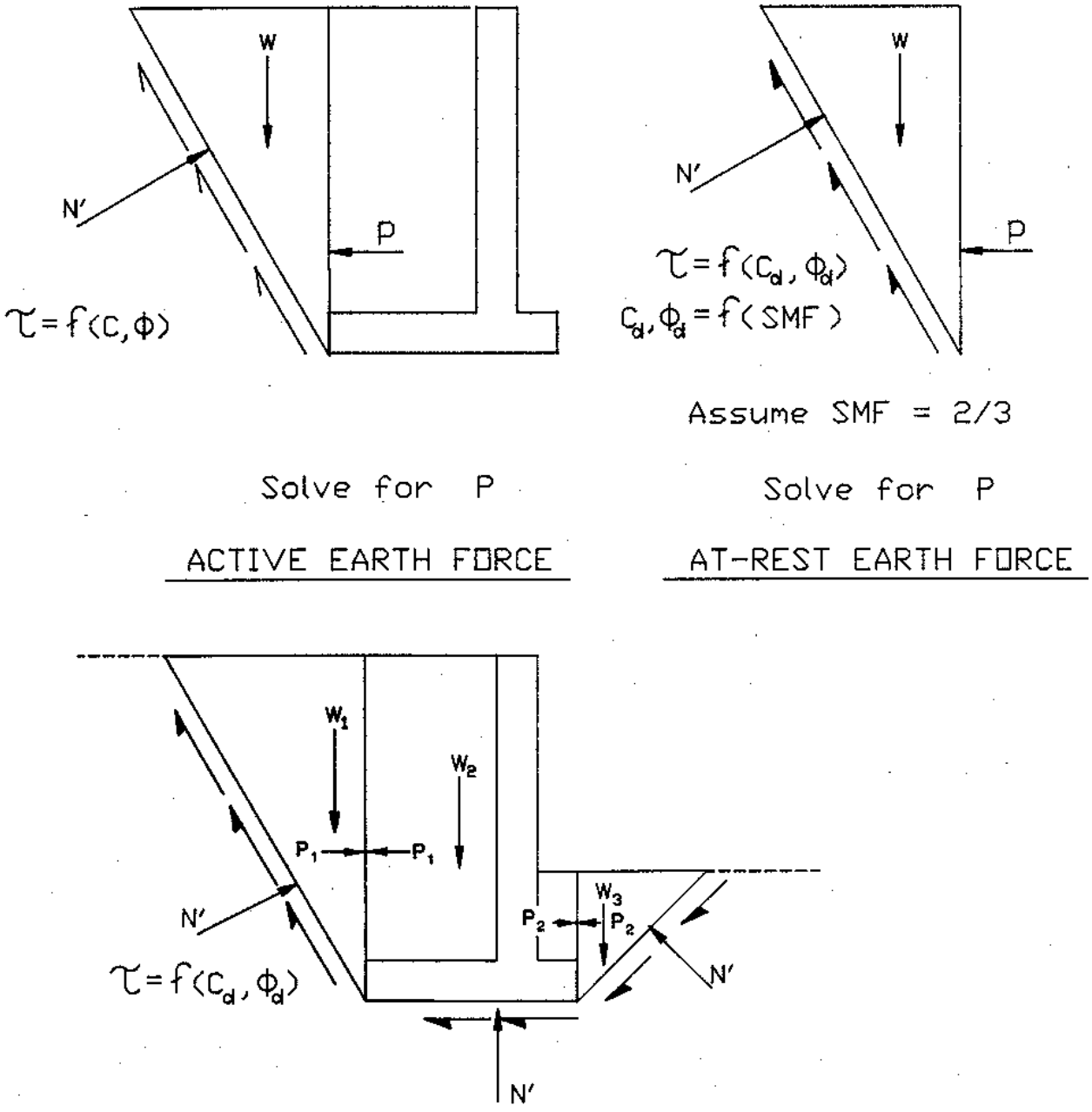

Figure 3-7. Application of the strength mobilization factor

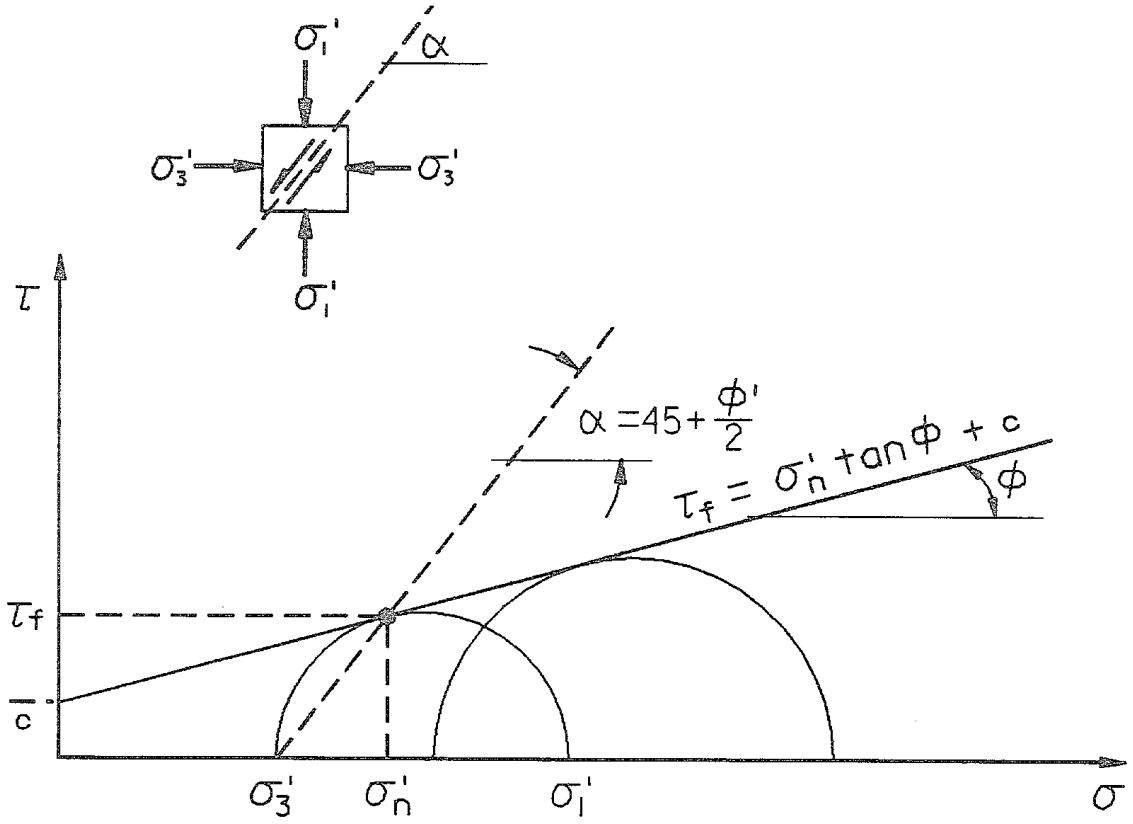

Figure 3-8. Mohr-Coulomb failure criterion

b. Developed Shear Stress. According to the Mohr-Coulomb failure criterion (Figure 3-8) the shear strength on the failure plane is defined as

$$\tau_f = \sigma'_n \tan \phi + c \qquad [3\text{-}8]$$

where

σ'_n = effective normal stress

ϕ, c = shear strength parameters of soil (where ϕ and c in the above equation are drained strengths ($\phi = \phi'$, $c = c'$) for long-term analysis and undrained ($\phi = 0$, $c = S_u$) for short-term analysis of cohesive materials).

The failure plane is inclined $45 + \phi/2$ degrees from the plane of the major principal stress. For limit-equilibrium analyses to be valid, the assumed slip surface must be inclined at this angle relative to the principal stresses. In the Coulomb and general wedge methods, a plane slip surface is assumed. Discontinuities in the backfill surface, surcharges, and wall friction all cause variation in the principal stress directions and induce

curvature in the slip surface. Assuming that the plane slip surface approximation is valid and is properly oriented relative to the principal stresses, the shear stress on it is:

$$\tau = SMF\ (c) + \sigma_n'\ SMF\ (\tan \phi) \qquad [3\text{-}9]$$

Thus, the shear stress on a presumed slip surface is taken to be a function of the shear strength parameters, the effective normal stress, and the strength mobilization factor.

c. Developed Shear Strength Parameters. Multiplying the shear strength parameters (c and $\tan \phi$) by the appropriate SMF reduces them to the "developed" values (c_d and $\tan \phi_d$) assumed to be operative in equilibrium conditions. The developed shear strength parameters, the actual shear strength parameters, and the SMF are related as follows:

$$SMF = \frac{\tan \phi_d}{\tan \phi} = \frac{c_d}{c} \qquad [3\text{-}10]$$

To estimate at-rest pressures for design using Coulomb's active earth pressure equation or the general wedge equation, the SMF should be taken as 2/3 (0.667). K_o values so obtained are compared with Jaky's equation in Figure 3-6. The Coulomb equation with an SMF of 2/3 is compared to the Danish Code and Jaky equations in Appendix E. It should be noted that as the ratio, $\tan \beta / \tan \phi$, exceeds 0.56, the lateral earth force computed by the Coulomb or general wedge equations using an SMF = 2/3 will be increasingly larger than that given by computing the earth force using a K_o given by the Danish Code equation, for those conditions where the Danish Code equation applies. Therefore, computing at-rest earth loadings using the Coulomb or general wedge equations for a sloping backfill when $\tan \beta / \tan \phi$ exceeds 0.56 will be conservative (see Appendix E).

3-12. Earth Force Calculation, Coulomb's Equations.

a. General.

(1) Coulomb's equations solve for active and passive earth forces by analyzing the equilibrium of a wedge-shaped soil mass. The mass is assumed to be a rigid body sliding along a plane slip surface. Design (at-rest) earth pressures and forces may be estimated using developed shear strength parameters (Equation 3-10) corresponding to an SMF of 2/3 in the Coulomb active earth force equation. The Coulomb equations have the advantage of providing a direct solution where the following conditions hold:

(a) There is only one soil material (material properties are constant). There can be more than one soil layer if all the soil layers are horizontal.

(b) The backfill surface is planar (it may be inclined).

(c) The backfill is completely above or completely below the water table, unless the top surface is horizontal, in which case the water table may be anywhere within the backfill.

(d) Any surcharge is uniform and covers the entire surface of the driving wedge.

(e) The backfill is cohesionless, unless the top surface is horizontal, in which case the backfill may be either cohesionless or cohesive.

(2) Although Coulomb's equation solves only for forces, it is commonly expressed as the product of a constant horizontal pressure coefficient K and the area under a vertical effective stress diagram. Assuming the concept of a constant K is valid, horizontal earth pressures can be calculated as the product of K times the effective vertical stress. The variation of the Coulomb solution from a more rigorous log-spiral solution is generally less than 10 percent, as shown in Figure 3-9.

b. Driving-Side Earth Force.

(1) The total active force P_A on a unit length of wall backfilled with a cohesionless material (c = 0) is given by:

$$P_A = \frac{1}{2} \gamma' \frac{1}{\sin \theta \cos \delta} K_A h^2 \qquad [3\text{-}11]$$

and acts at an angle δ from a line normal to the wall. In the above equation (refer to Figure 3-10):

γ' = effective unit weight (moist or unsaturated unit weight if above the water table, submerged or buoyant unit weight if below the water table)

θ = angle of the wall face from horizontal (90 degrees for walls with a vertical back face or structural wedge)

δ = angle of wall friction

K_A = active earth pressure coefficient

h = height of fill against gravity wall or height of fill at a vertical plane on which the force is being computed

where

$$K_A = \frac{\sin^2 (\theta + \phi) \cos \delta}{\sin \theta \sin (\theta - \delta) \left[1 + \sqrt{\frac{\sin (\phi + \delta) \sin (\phi - \beta)}{\sin (\theta - \delta) \sin (\theta + \beta)}} \right]^2} \qquad [3\text{-}12]$$

Examples 1 and 2 in Appendix M and the examples in Appendix N demonstrate the use of Equation 3-12.

(2) When wall friction is neglected ($\delta = 0$), Equation 3-12 reduces to:

$$K_A = \frac{\sin^2 (\theta + \phi)}{\sin^2 \theta \left[1 + \sqrt{\frac{\sin \phi \sin (\phi - \beta)}{\sin \theta \sin (\theta + \beta)}} \right]^2} \qquad [3\text{-}13]$$

(3) For the case of is no wall friction ($\delta = 0$) and a vertical wall ($\theta = 90$ degrees),

$$K_A = \frac{\cos^2 \phi}{\left[1 + \sqrt{\frac{\sin \phi \sin (\phi - \beta)}{\cos \beta}} \right]^2} \qquad [3\text{-}14]$$

(4) For the special case of no wall friction, horizontal backfill surface, and a vertical wall, Coulomb's equation for K_A reduces to:

$$K_A = \frac{1 - \sin \phi}{1 + \sin \phi} = \tan^2 \left(45° - \frac{\phi}{2} \right) \qquad [3\text{-}15]$$

which is identical to Rankine's equation for this special case.

(5) As stated in paragraph 3-11c and demonstrated in Figure 3-6 and Appendix E, a developed ϕ angle computed by Equation 3-10 using an SMF of 2/3 can be used in Coulomb's equation to compute an earth pressure coefficient close to that given by the Jaky or Danish Code equations.

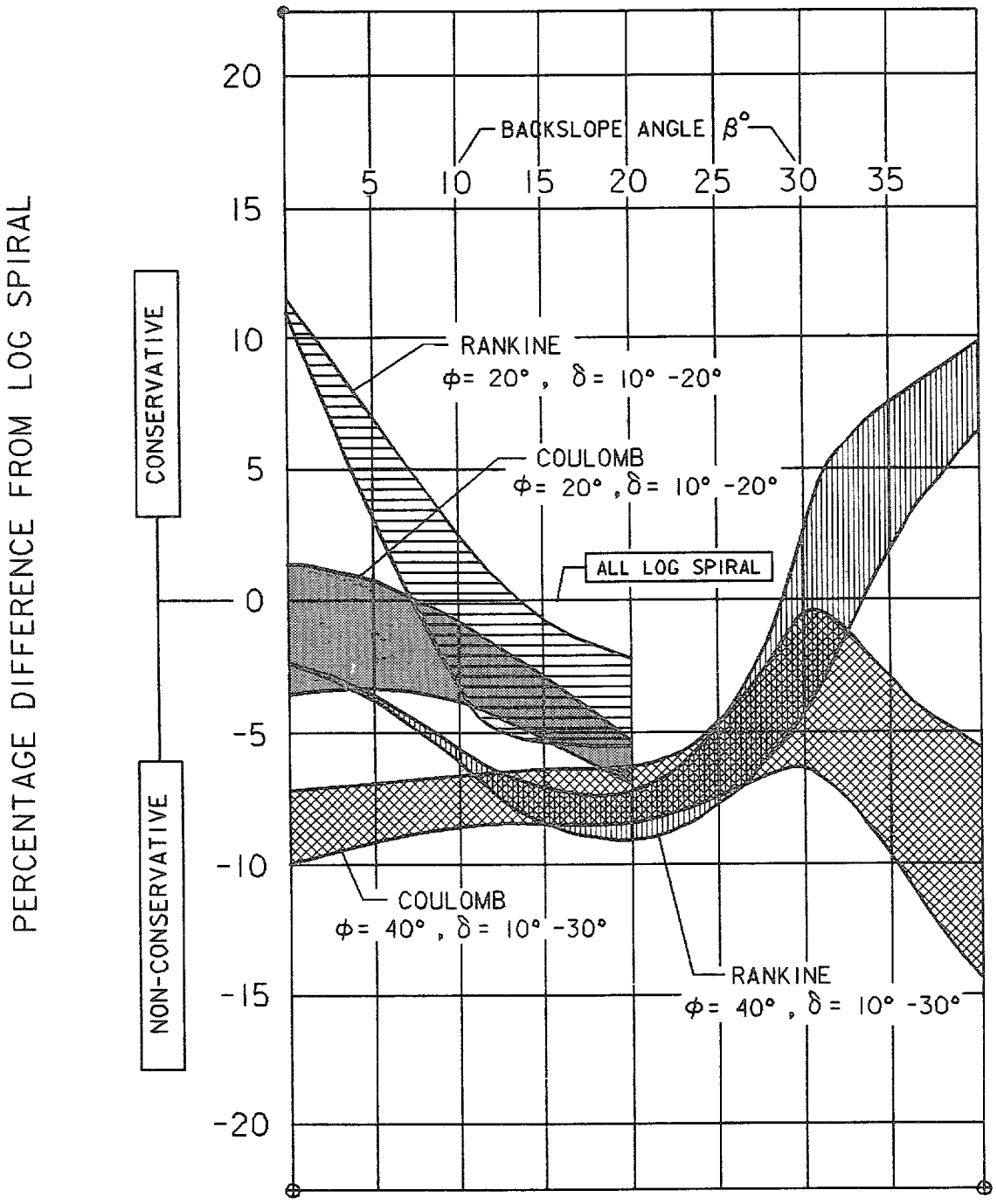

NOTE: Log spiral calculations based upon Caquot and Kerisel coefficients. Range of values for Rankine is from influence of wall friction on log spiral.

Figure 3-9. Comparison of active earth pressures (after Driscoll 1979)

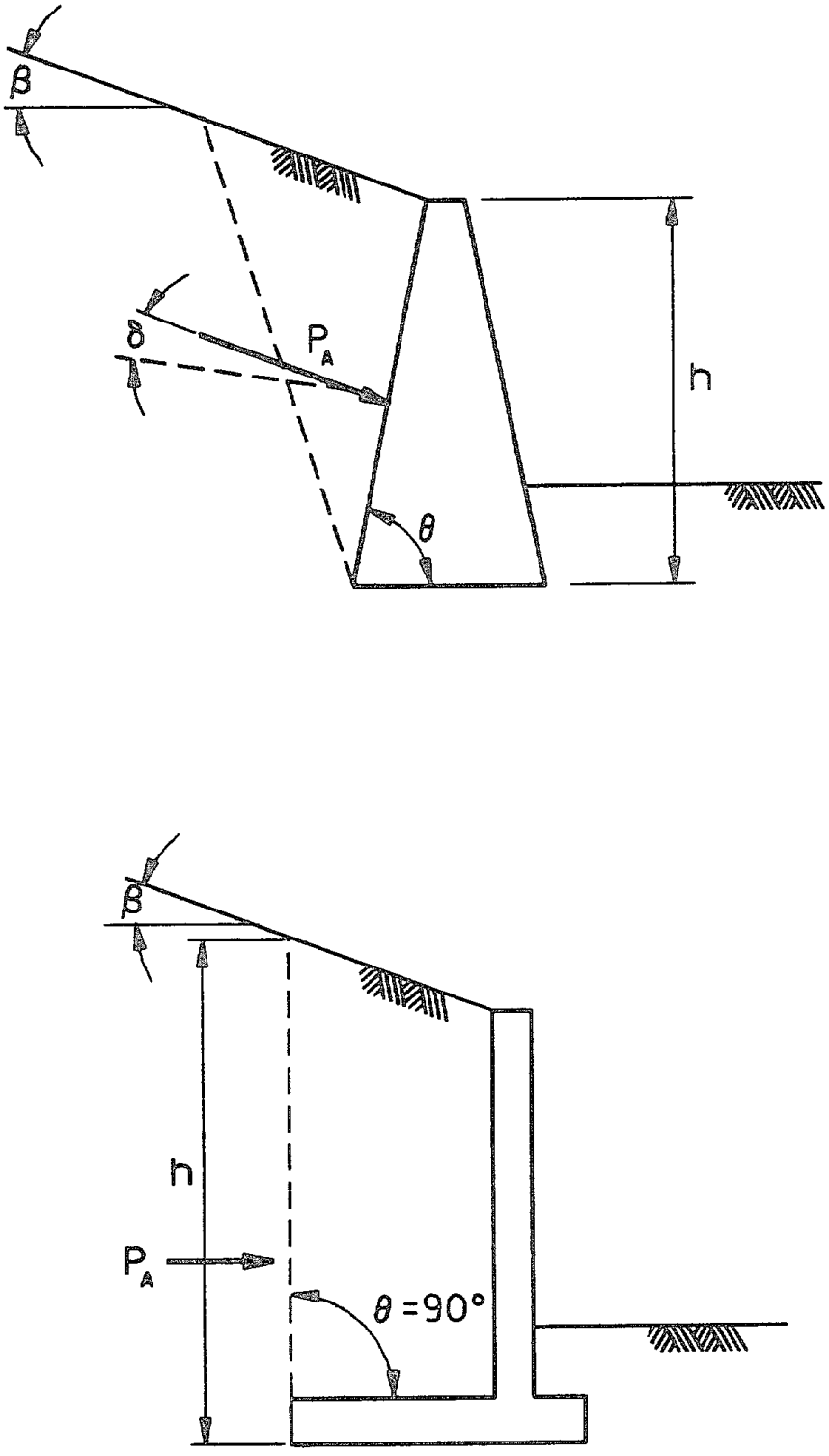

Figure 3-10. Variables used in Coulomb equation

(6) For the horizontal component of the earth force acting on a vertical plane, with no wall friction, the term (1/sin θ cos δ) in Coulomb's equation is equal to unity. Thus, Equation 3-11 reduces to

$$P_{AH} = \left(\frac{1}{2}\right) K_A \gamma' h^2 \qquad [3-16]$$

(7) If total stress or undrained strength parameters are used and there is a cohesion term c it has the effect of reducing the active earth force P_{AH} :

$$P_{AH} = \left(\frac{1}{2}\right) K_A \gamma' h^2 - 2c\sqrt{K_A}\, h + \frac{2c^2}{\gamma'} \qquad [3-17]$$

For a backfill with a horizontal surface, K_c given in Appendix H, paragraph H-2c, equals $\sqrt{K_A}$. The second term is the reduction in the active force due to the effect of cohesion on the slip plane and the third term accounts for the shortened length of slip plane due to the effect of a tension crack. If the third term is neglected, and K is assumed constant with depth, the active pressure can be obtained as the derivative of P_{AH} with respect to the depth from the top of the wall z :

$$p_{AH} = K_A \gamma' z - 2c\sqrt{K_A} \qquad [3-18]$$

Refer to examples 5 and 8 of Appendix M for examples involving cohesion.

(8) Estimation of at-rest pressures using the SMF concept with Coulomb's equation may give unreliable results for medium to highly plastic cohesive materials. If these materials cannot be avoided in the area of the driving side wedge, the at-rest pressure should be taken as the overburden pressure times as empirical K value, such as from Massarsch's (1979) or Brooker and Ireland's (1965) correlation of K with the plasticity index. Because of the number of uncertainties about the behavior of cohesive materials, a degree of conservatism should be exercised in the selection of the K values. Also, the effects of short and long term conditions (paragraph 3-5c) and compaction (paragraph 3-17) should be included in estimating the at-rest pressure.

c. Resisting-Side Earth Force.

(1) The Coulomb and general wedge equations assume a plane slip surface. However, wall friction effects cause the actual slip surface at failure to be curved. For active pressure calculations, the magnitude of error introduced by the plane surface assumption is not significant, as shown in Figure 3-9 (Driscoll 1979). Coulomb's passive force equation, however, is grossly unconservative where wall friction is present as shown in Figure 3-11 (Driscoll 1979). However, where δ is less than about one-third ϕ, the error is small. If wall friction is neglected, Coulomb's equation is therefore acceptable. The Coulomb passive pressure coefficient for the case of no wall friction ($\delta = 0$) and a vertical wall ($\theta = 90$ degrees) is:

$$K_P = \frac{\cos^2 \phi}{\left[1 - \sqrt{\frac{\sin \phi \sin (\phi + \beta)}{\cos \beta}}\right]^2} \qquad [3\text{-}19]$$

For a horizontal backfill ($\beta = 0$), this reduces to

$$K_P = \frac{1 + \sin \phi}{1 - \sin \phi} = \tan^2 \left(45° + \frac{\phi}{2}\right) = \frac{1}{K_A} \qquad [3\text{-}20]$$

(2) If total stress or undrained strength parameters are used and there is a cohesion term c, it has the effect of increasing the passive earth force p_{PH}:

$$p_{PH} = \frac{1}{2} K_P \gamma' h^2 + 2c\sqrt{K_P}\, h \qquad [3\text{-}21]$$

By differentiating p_{PH} with respect to the depth from the top of the resisting wedge z, the passive pressure may be obtained as:

$$p_{PH} = K_P \gamma' z + 2\sqrt{K_P}\, c \qquad [3\text{-}22]$$

3-13. Earth Force Calculation, General Wedge Method.

a. General. The general wedge method refers to a limit equilibrium analysis of a set of assumed rigid bodies (soil and/or structural elements)

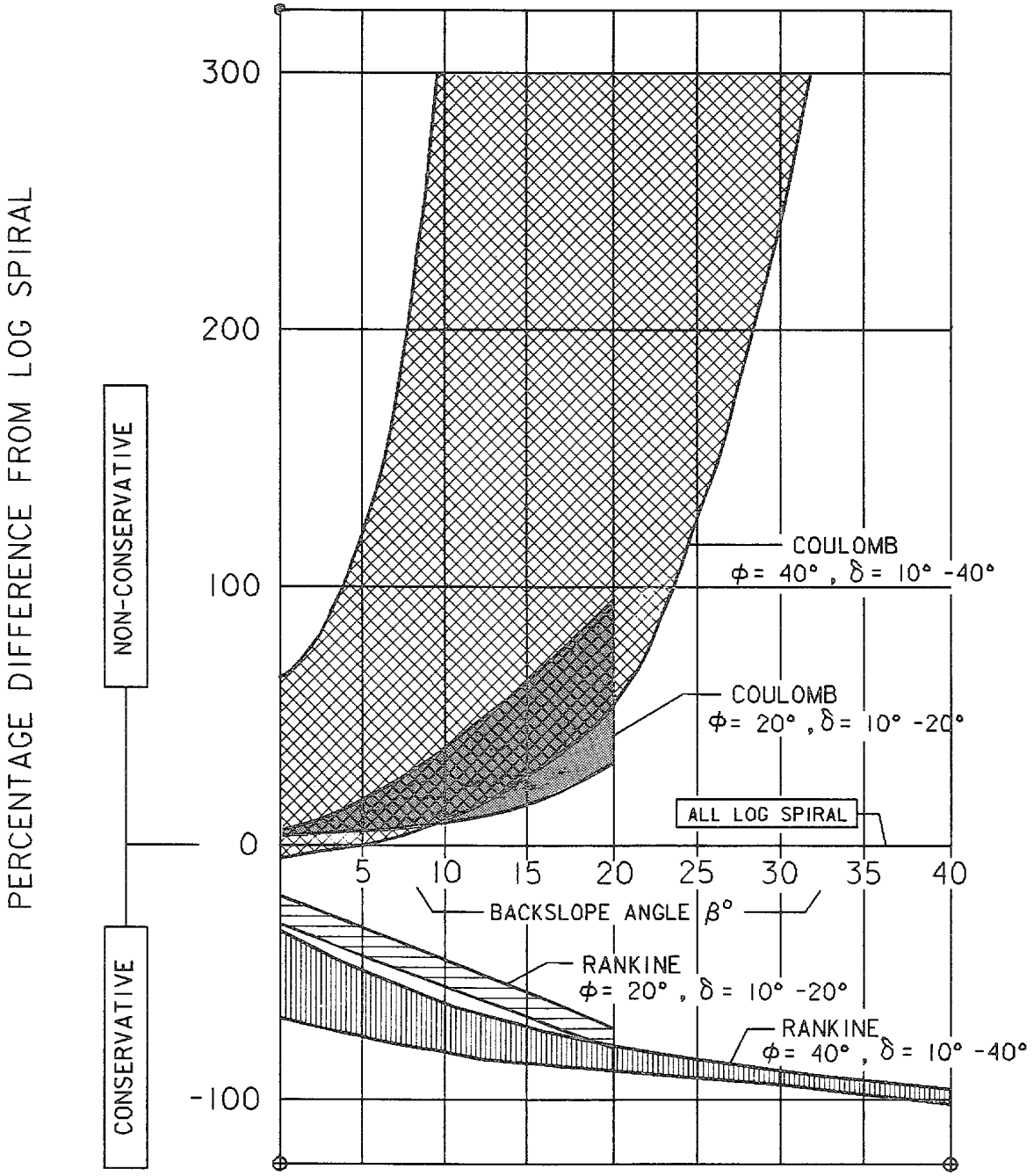

NOTE: Log spiral calculations based upon Caquot and Kerisel coefficients.

Figure 3-11. Comparison of passive earth pressures (after Driscoll 1979)

termed wedges. The horizontal earth force on the driving or resisting side of a retaining structure may be estimated by such an analysis employing properly chosen strength parameters. Where the special conditions listed in paragraph 3-12a(1) apply, the weight of the sliding mass and orientation of the critical sliding plane are unique functions of the backfill geometry and soil properties, and Coulomb's equations provide direct solutions for the driving and resisting earth forces. Where one or more of the variables in Coulomb's equation cannot be accommodated as a single value (such as the case with multiple soils where not all of the soil layers are horizontal, location of the water table, irregular backfills or where nonuniform surcharges are present), the critical inclination of the sliding surface and, in turn, the gravity forces (weight plus surcharges) on the sliding mass must be solved in order to calculate the horizontal earth force. In these cases, this requires a trial and error solution using the general wedge equation.

b. Use in Practice. When used with unfactored soil strength parameters, the general wedge equations yield the active and passive earth forces. When c and tan ϕ are factored by an SMF value of 2/3, solution of the driving-side wedge provides an estimate of the at-rest earth forces (see paragraph 3-12). An SMF of 2/3 is not used to compute the resisting wedge force for the overturning, bearing, and structural design of the wall since a larger resisting force than is acceptable would be computed. See paragraph 3-8 for the procedure recommended to determine the resisting force for overturning and bearing capacity analyses and structural design of the wall.

c. Driving Side Earth Force, General Wedge Method.

(1) Wedge Geometry and Forces. The geometry of a typical driving-side wedge and its free-body diagram are shown in Figure 3-12. The angle of wall friction and the shear force between vertical wedge boundaries are assumed to be zero. The inclination of the slip surface α is that which maximizes the earth force. Calculation of α is discussed in paragraphs 3-13c(2) and 3-13c(4). If force equilibrium is satisfied, the forces on the wedge form a closed-force polygon as shown in Figure 3-13. The equation for the effective horizontal earth force P_{EE} exerted by a driving-side wedge on a wall or an adjacent wedge is given by the general wedge equation as:

$$P_{EE} = \frac{(W + V)\ (1 - \tan \phi_d \cot \alpha)\ \tan \alpha}{1 + \tan \phi_d \tan \alpha} + \frac{U \tan \phi_d - c_d L}{\cos \alpha\ (1 + \tan \phi_d \tan \alpha)}$$

$$+ H_L - H_R - P_W \qquad [3\text{-}23]$$

where

P_{EE} = effective horizontal earth force contributed by wedge or wedge segment

W = total wedge weight, including water

V = any vertical force applied to wedge

α = angle between slip plane and horizontal

U = uplift or buoyancy force acting on and normal to wedge slip plane

L = length along the slip plane of the wedge

H_L = any external horizontal force applied to the wedge from the left, acting to the right

H_R = any external horizontal force applied to the wedge from the right, acting to the left

P_W = internal water force acting on the side of the wedge free body (P_W is equal to the net difference of the water force for wedge segments with water on two vertical sides as shown in Figures 3-12 and 3-13.)

The developed strength parameters $\tan \phi_d$ and c_d are as defined in paragraph 3-11. Equation 3-23 is derived for failure occurring from left to right. All values are positive in the directions indicated in Figure 3-12. Refer to Appendix M for examples using Equation 3-23.

(2) Critical Value of Slip-Plane Angle.

(a) The critical value of α for a driving-side wedge with a horizontal top surface and a uniform surcharge or no surcharge is:

$$\alpha = 45° + \frac{\phi_d}{2} \qquad [3\text{-}24]$$

(b) For the special case of a backfill with a planar (flat or inclined) top surface and a strip surcharge V, the following equation can be used to compute the critical α value:

$$\alpha = \tan^{-1}\left(\frac{c_1 + \sqrt{c_1^2 + 4c_2}}{2}\right) \qquad [3\text{-}25]$$

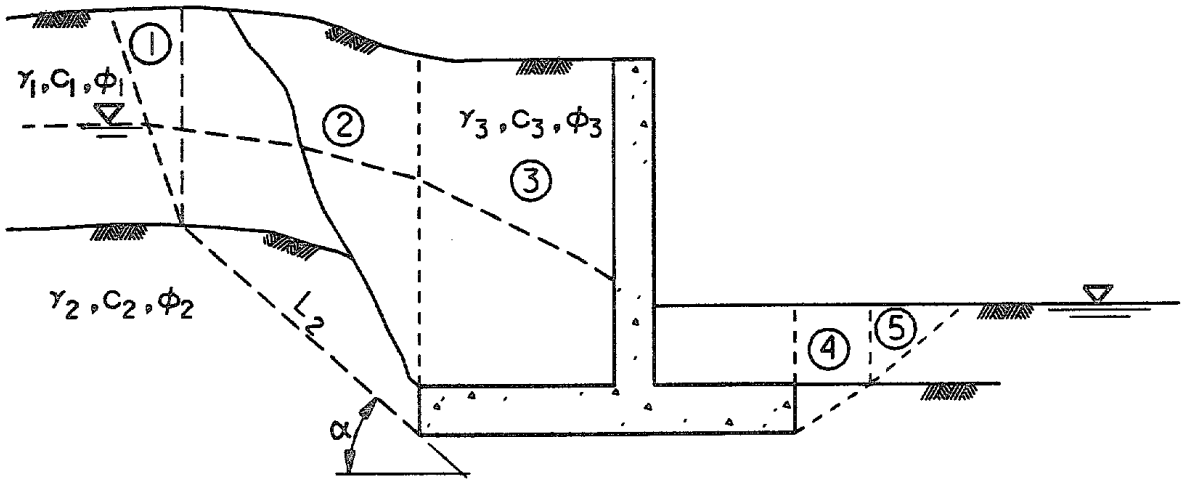

a. Estimation of forces using slices

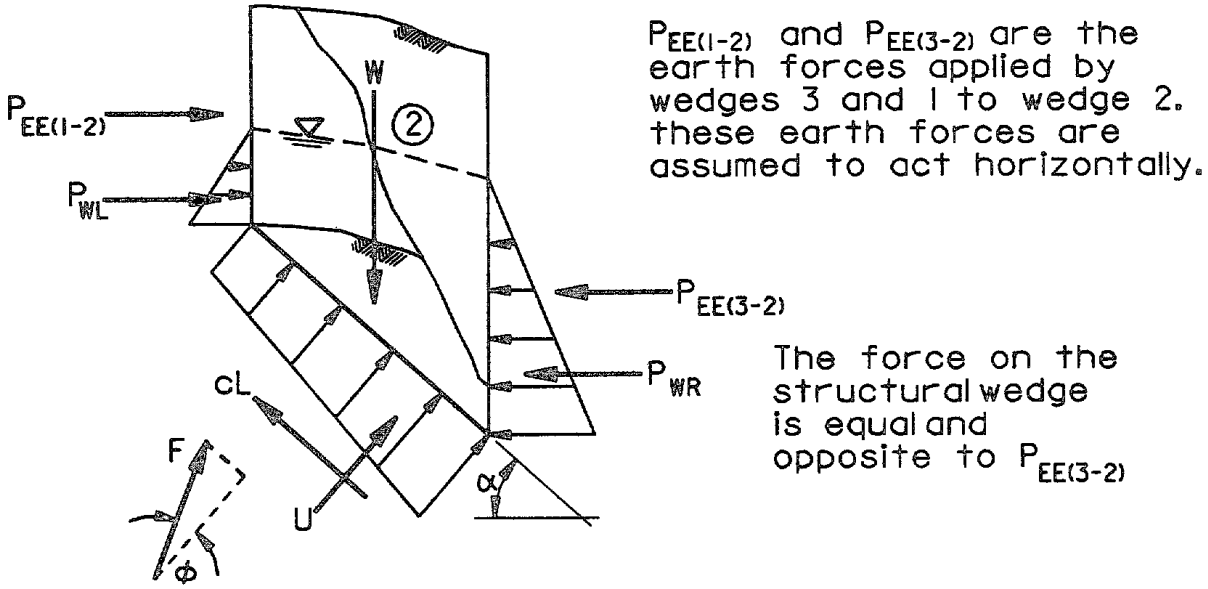

b. Free body of wedge 2

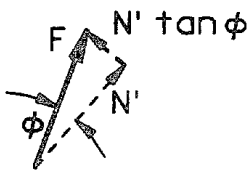

c. Derivation of force F

Figure 3-12. Wedge method on driving side

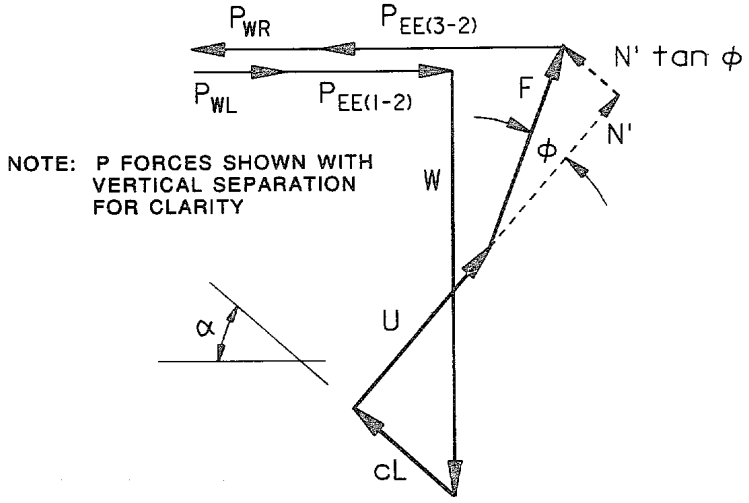

Force on driving side of structural wedge (slice 3) is equal and opposite to $P_{EE(3-2)}$. The force P_{EE} added by the wedge is ($P_{EE(3-2)} - P_{EE(1-2)}$) and acts to the right. The force P_w is equal to $P_{WR} - P_{WL}$ and acts to the right.

Figure 3-13. Force polygon for wedge method on driving side

The above equation for α assumes that the backfill is completely above or completely below the water table, but can be used when the water table is anywhere within the backfill with sufficient accuracy for design. The surcharge V can have any arbitrary shape but must be contained entirely within the driving wedge. The equations for c_1 and c_2 are:

(i) For a cohesionless backfill without a strip surcharge:

$$c_1 = 2 \tan \phi_d \qquad [3\text{-}26]$$

$$c_2 = 1 - \tan \phi_d \tan \beta - \left(\frac{\tan \beta}{\tan \phi_d} \right) \qquad [3\text{-}27]$$

(ii) For a cohesive or a cohesionless backfill with a strip surcharge:

$$c_1 = \frac{2 \tan^2 \phi_d + \frac{4c_d (\tan \phi_d + \tan \beta)}{\gamma(h + d_c)} - \frac{4V \tan \beta\left(1 + \tan^2 \phi_d\right)}{\gamma\left(h^2 - d_c^2\right)}}{A} \qquad [3\text{-}28]$$

$$c_2 = \frac{\tan \phi_d (1 - \tan \phi_d \tan \beta) - \tan \beta + \frac{2c_d(1 - \tan \phi_d \tan \beta)}{\gamma(h + d_c)} + \frac{2V \tan^2 \beta\left(1 + \tan^2 \phi_d\right)}{\gamma\left(h^2 - d_c^2\right)}}{A} \qquad [3\text{-}29]$$

where

$$A = \tan \phi_d + \frac{2c_d(1 - \tan \phi_d \tan \beta)}{\gamma(h + d_c)} - \frac{2V\left(1 + \tan^2 \phi_d\right)}{\gamma\left(h^2 - d_c^2\right)} \qquad [3\text{-}30]$$

These equations when applied to a cohesive backfill are subject to the limitations described in paragraph 3-12b(8). The derivation of these equations is shown in Appendix G. Examples using these equations are shown in Appendix M.

(c) For irregular backfills, obtaining the critical inclination of the driving-side slip surface may require a trial-and-error solution. As a first approximation, the backfill surface may be bounded by two inclined lines originating from the top of the wall and the value of α may be calculated using an "average" β value between the two bounding lines (Figure 3-14), or by introducing a surcharge as shown in Example 9 of Appendix M.

(3) Limitations of Critical Slip Plane Equations. The equations for c_1 and c_2 are valid except when the strip surcharge V is too large or when the slope of the top surface is too great. The maximum value for the strip

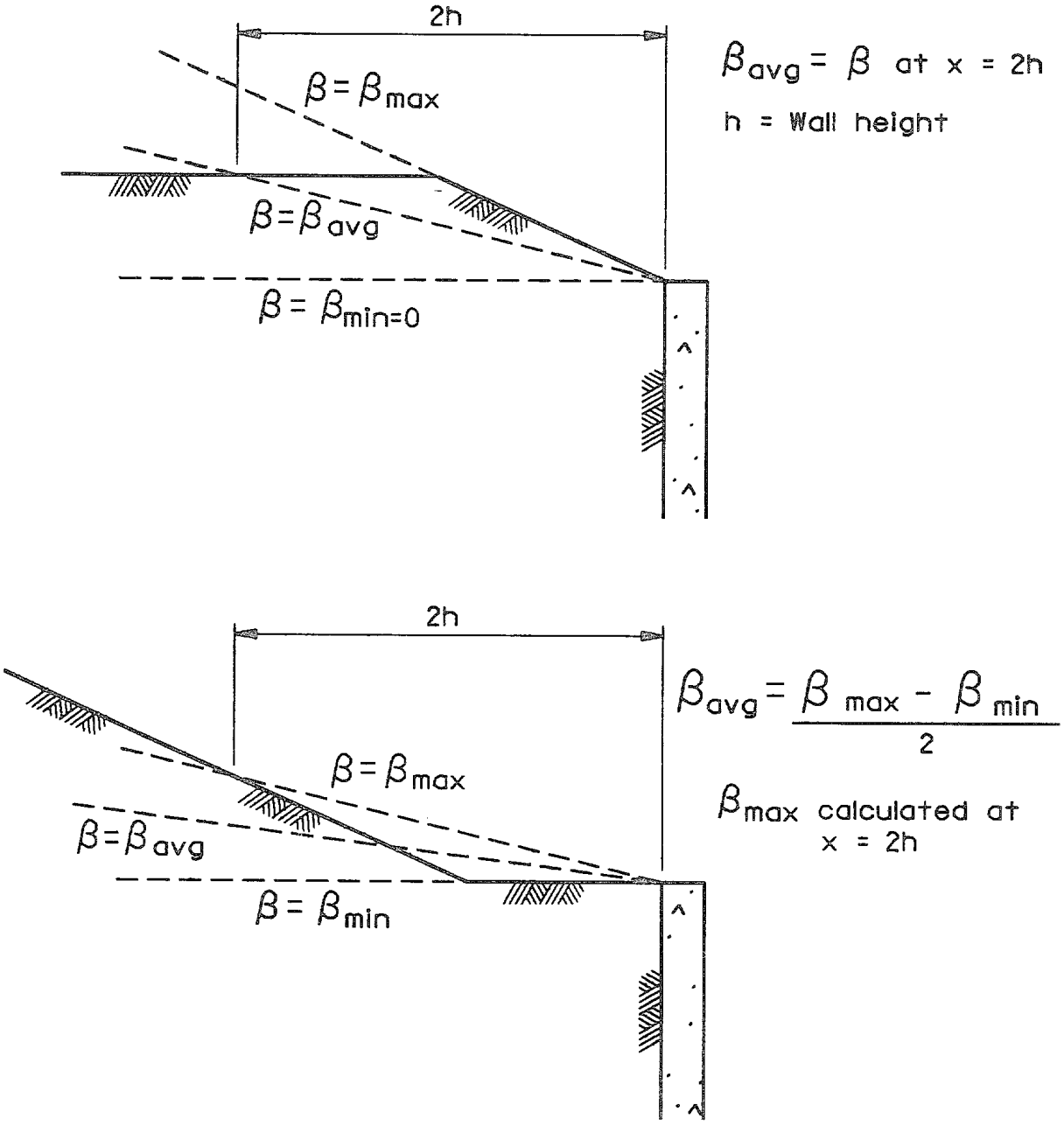

Figure 3-14. Wedge analysis for irregular backfill

surcharge is determined by setting the denominator of the equation for c_1 or c_2 equal to zero and solving for V. This value is:

$$ax = \frac{\gamma\left(h^2 - d_c^2\right) \tan \phi_d + 2c_d(h - d_c)(1 - \tan \phi_d \tan \beta)}{2\left(1 + \tan^2 \phi_d\right)} \qquad [3-3$$

When $V \geq V_{max}$ the value of α is set by the location of the strip surcharge as shown in Figure 3-15, and given by the equation

$$|\alpha| = \tan^{-1} \frac{h - d_c + (S) \tan \beta}{S} \qquad [3-32]$$

Even when $V < V_{max}$, a check should be made to be certain that the entire strip surcharge lies on the top surface of the wedge as defined by the calculated value of α. Also, when $c_1^2 + 4c_2 < 0$, α is indeterminate. This is an indication that the slope of the top surface is too great to be sustained by the developed strength parameters $\tan \phi_d$ and c_d. See example 8 in Appendix M for a solution to this problem.

(4) Layered Soils. The wedge equations imply a single set of strength parameters along the wedge base. For layered soils, the wedge must be divided into wedge segments, each with its base in a single soil. The wedge base inclinations α are theoretically different in every soil (Figure 3-16a); calculation of an optimum solution (maximized earth force) for the set of α values is tedious and cumbersome. Three approximate methods may be used:

(a) The critical inclination in each layer may be calculated according to Equation 3-25 using the developed shear strength parameters for the soil along the wedge base and using the slope angle β at the top of each wedge segment (see Figure 3-16a).

(b) The wedge segment bases may be assumed to have a constant inclination α through all materials and the critical value (corresponding to the maximum driving side force) may be calculated by trial using Equation 3-23 (see Figure 3-16b).

(c) Alternatively, the critical slip-plane angle may be calculated (for each layer below the top layer) by using the procedure presented in paragraph G-7 of Appendix G (see example 6 in Appendix M).

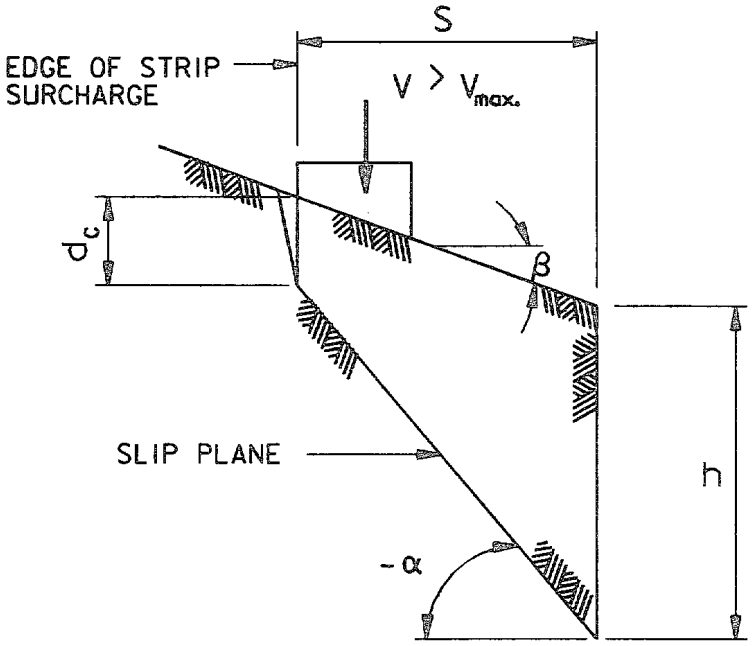

$$S = \frac{h - d_c}{\tan\alpha - \tan\beta}$$

$$\tan\alpha = \frac{h - d_c}{S} + \tan\beta = \frac{h - d_c + S\tan\beta}{S}$$

$$|\alpha| = \tan^{-1} = \left(\frac{h - d_c + S\tan\beta}{S}\right)$$

Figure 3-15. Surcharge effect on critical slip plane

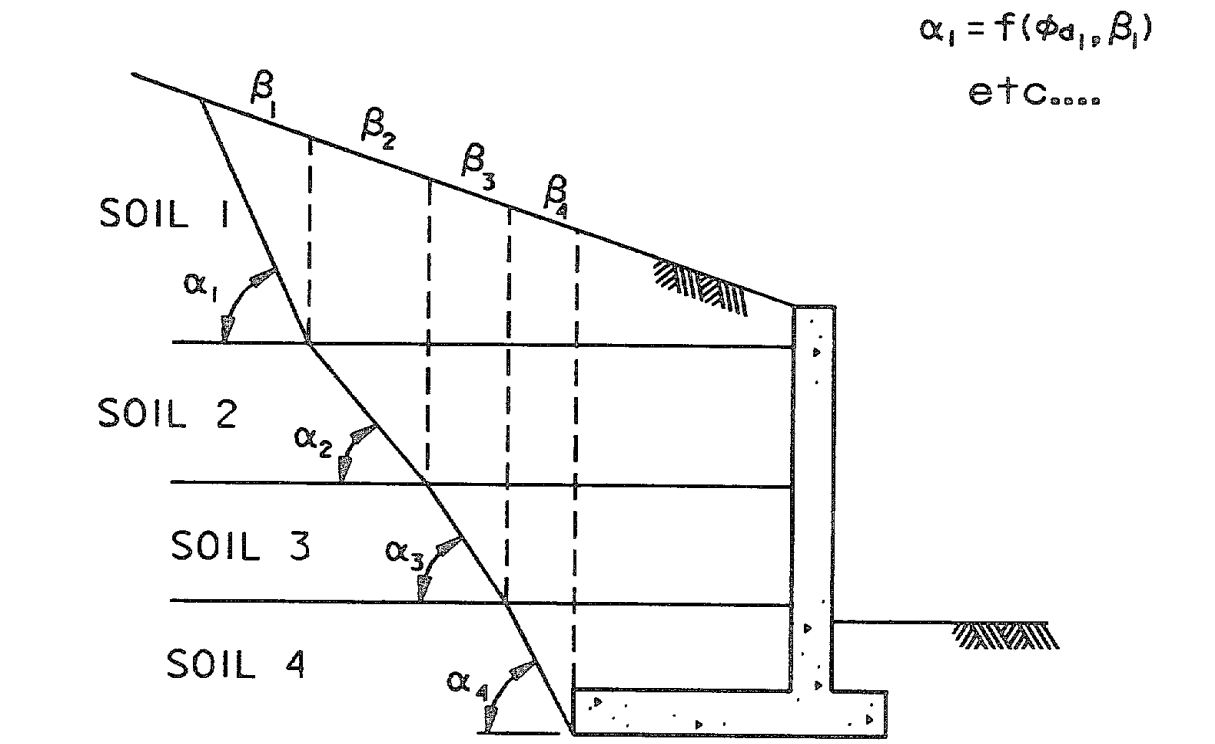

a. Wedge 1

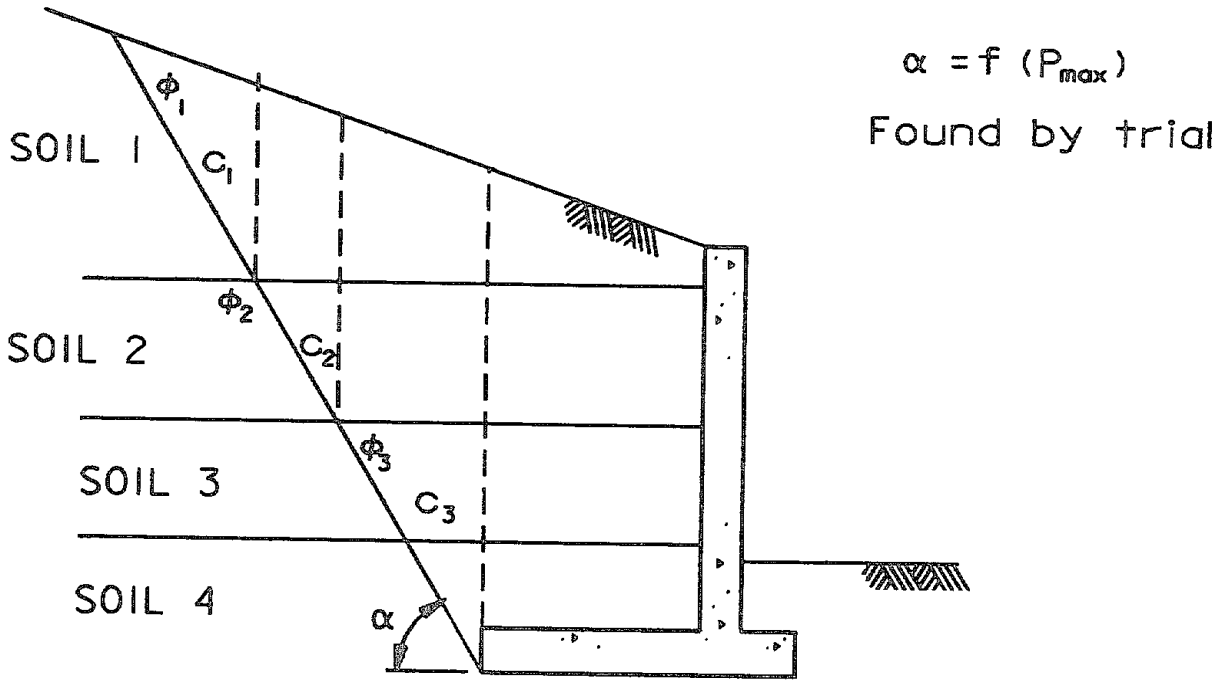

b. Wedge 2

Figure 3-16. Wedge analysis in layered soil

If the surfaces of all layers are horizontal, the critical slip plane may be determined using Equation 3-24.

(5) Surcharges. The wedge method incorporates surcharge effects into the resultant earth force if the surcharge force is added to the wedge weight. However, it is preferable to calculate horizontal pressures due to surcharges separately for the following reasons:

(a) The presence of a nonuniform surcharge alters the principal stress directions, increasing the curvature of the slip surface, and increasing the error associated with assuming a plane surface.

(b) Stresses induced by surcharges are distributed throughout a soil mass in a manner that may considerably alter the point of application and distribution of earth pressure as further described in paragraph 3-16. Limit-equilibrium techniques and the earth pressure coefficient concept do not accurately predict such distributions.

(c) The additional pressures developed on the wall depend on the amount of wall movement and may be twice as great for nonyielding walls as for yielding walls.

The intent of this manual is to consider walls to be relatively rigid and to design for at-rest conditions. Therefore, pressures and forces due to non-uniform surcharges should be calculated in accordance with paragraph 3-16, adding the results to the pressures and/or forces obtained from Coulomb’s equation or the general wedge equation. For the sliding analysis, surcharge effects may be included directly in the wedge method weight calculations because the sliding analysis considers only force equilibrium; thus, the point of application of the forces does not matter. Examples 4 and 10 of Appendix M demonstrate the calculation of horizontal pressures involving surcharges.

(6) Pressure Coefficients.

(a) Structural engineers are familiar with the use of Coulomb’s equations (paragraph 3-12) for the determination of earth pressure coefficients and the use of these coefficients in determining pressures and forces acting on retaining walls. These equations suffer from several limitations as discussed in paragraph 3-12a(1). The general wedge equation (Equation 3-23) is not subject to any of the limitations of Coulomb’s equations and may be used to solve for the lateral earth force on a wedge due to complicated geometry and surface loading. If lateral earth pressure coefficients are derived from the general wedge equation, these coefficients may be used in a rather simple manner to solve complex earth pressure problems.

(b) Earth pressures can be calculated from general wedge method solutions by assuming that pressures vary in a piecewise linear fashion and that the slopes of the pressure diagrams are the product of densities and pressure coefficients (K). The slopes may be considered the density of an "equivalent fluid" loading the wall. These pressure coefficients are dependent on the

problem geometry and are derived in Appendix H. It should be noted that pressure coefficients (K values) below the water table may differ from those above the water table in the same material as shown in Appendix H. One example where the K value is different above and below the water table is the case of a sloping backfill. Examples using pressure coefficients are shown in Appendix M.

d. Resisting Side Earth Force, General Wedge Method.

(1) Wedge Geometry and Forces. The geometry of a typical resisting-side wedge and its free-body diagram are shown in Figure 3-17. The angle of wall friction and the shear force between vertical wedge boundaries are assumed to be zero. The inclination of the slip surface α is that which minimizes the earth force. Calculation of α is discussed in paragraph 3-13d(2). If force equilibrium is satisfied, the forces on the wedge form a closed force polygon as shown in Figure 3-17. The equation for the horizontal effective earth force P_{EE} exerted by a resisting-side wedge on a wall or an adjacent wedge is:

$$P_{EE} = \frac{(W + V)(1 + \tan \phi_d \cot \alpha) \tan \alpha}{1 - \tan \phi_d \tan \alpha} - \frac{U \tan \phi_d - c_d L}{\cos \alpha \, (1 - \tan \phi_d \tan \alpha)}$$

$$- H_L + H_R - P_W \qquad [3\text{-}33]$$

where the terms are the same as for the driving-side wedge equation (Equation 3-23). Equation 3-33 is derived for failure occurring from left to right. All values are positive in the directions indicated in Figure 3-17.

(2) Critical Value of Slip-Plane Angle.

(a) For a resisting-side wedge with a horizontal top surface, α can be computed as follows:

$$\alpha = 45° - \frac{\phi_d}{2} \qquad [3\text{-}34]$$

(b) The critical angle α for a resisting-side wedge with a planar (flat or inclined) top surface, with no surcharge or with a strip surcharge V , is given by the equation:

$$\alpha = \tan^{-1}\left[\frac{-c_1 + \sqrt{c_1^2 + 4c_2}}{2}\right] \qquad [3\text{-}35]$$

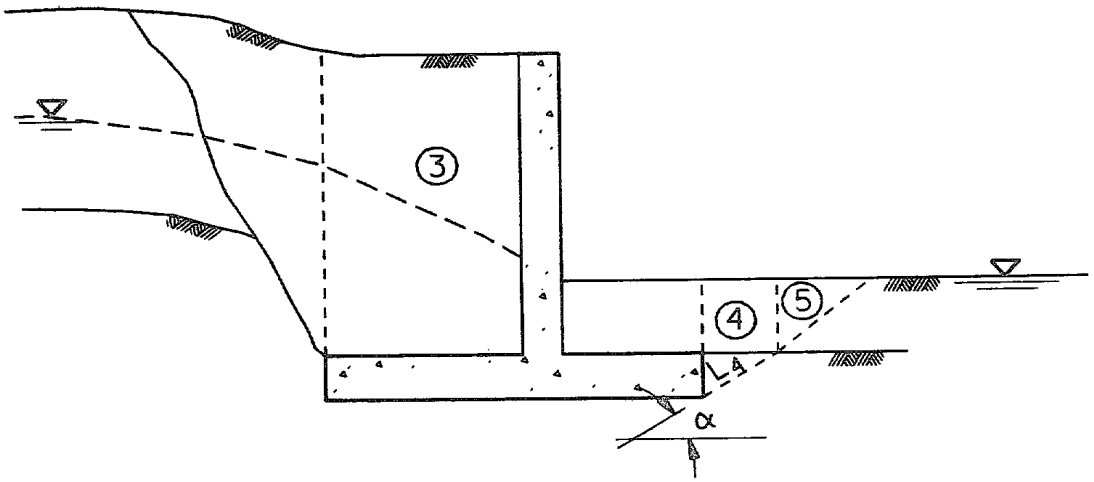

a. Estimation of forces using slices

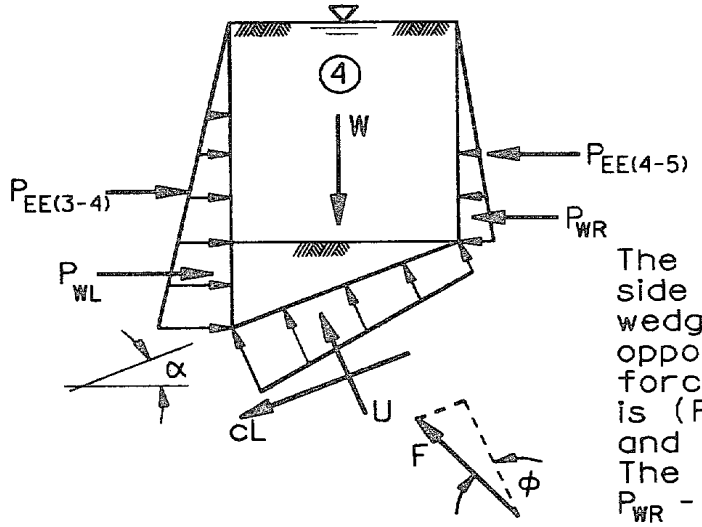

The force on the resisting side of the structural wedge is equal and opposite to $P_{EE(3-4)}$. The force P_{EE} added by the wedge is $(P_{EE(3-4)} - P_{EE(4-5)})$ and acts to the left. The force P_W is equal to $P_{WR} - P_{WL}$ and acts to the left.

b. Free-body diagram of slice 4

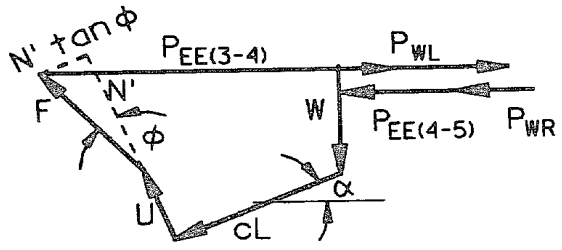

c. Force polygon for slice 4

Figure 3-17. Wedge method for resisting-side wedge

For a resisting-side wedge, the equations for c_1 and c_2 are

$$c_1 = \frac{2 \tan^2 \phi_d + \frac{4c_d (\tan \phi_d - \tan \beta)}{\gamma h} - \frac{4V \tan \beta \left(1 + \tan^2 \phi_d\right)}{\gamma h^2}}{A} \qquad [3\text{-}36]$$

$$c_2 = \frac{\tan \phi_d (1 + \tan \phi_d \tan \beta) + \tan \beta + \frac{2c_d (1 + \tan \phi_d \tan \beta)}{\gamma h} - \frac{2V \tan^2 \beta \left(1 + \tan^2 \phi_d\right)}{\gamma h^2}}{A} \qquad [3\text{-}37]$$

$$A = \tan \phi_d + \frac{2c_d (1 + \tan \phi_d \tan \beta)}{\gamma h} + \frac{2V \left(1 + \tan^2 \phi_d\right)}{\gamma h^2} \qquad [3\text{-}38]$$

(3) Surcharges. The comments regarding surcharges in paragraph 3-13c(5) relative to analysis of driving-side wedges also apply in general to resisting-side wedges. However, surcharges on resisting-side wedges tend to enhance stability and therefore it is conservative to neglect them in analysis. If resisting-side surcharges are not neglected, it must be assured that the surcharge loading will be in place for the condition analyzed.

(4) Pressure Coefficients. Earth pressures for the resisting side may be calculated as equivalent fluid pressures in a manner similar to that for the driving side. See paragraph 3-13c(6) and Appendix H for further discussion.

3-14. Earth Pressure Calculations Including Wall Friction.

a. Driving Side. Friction between the backfill and wall, or on a plane within the backfill, of up to one-half of the internal friction angle (unfactored) of the backfill material may be used in the design.

b. Resisting Side. When wall friction is included in the analysis, assuming the slip surface to be a log-spiral or other curved surface provides lower and more reasonable values for the passive force and passive pressure coefficient K_P (see Figure 3-11). Although the angle of wall friction should generally be taken as zero, it may be assumed greater than zero where movement and settlement of the wall are expected and permissible. Figure 3-18 provides earth pressure coefficients for horizontal backfills based on the work of Caquot and Kerisel (1948) and Shields and Tolunay (1973).

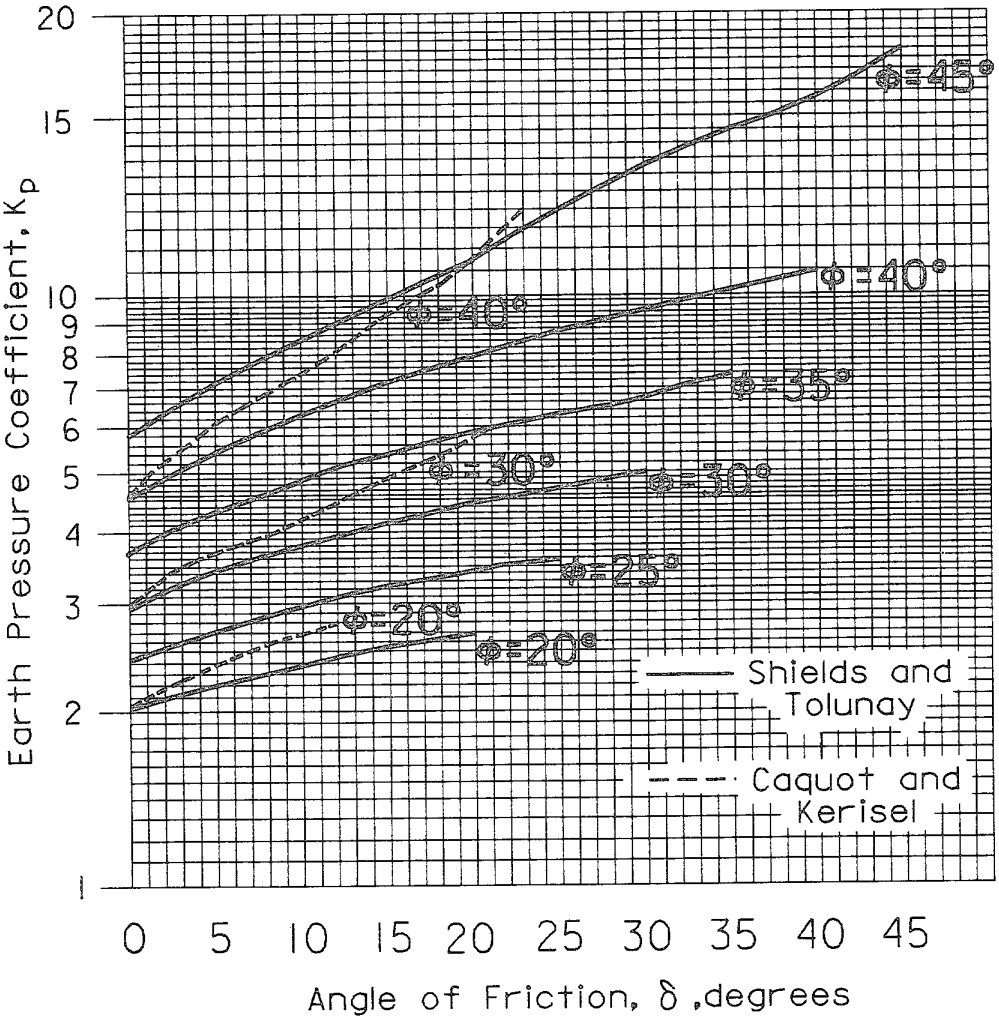

Figure 3-18. Passive earth pressure coefficients

3-15. Distribution of Horizontal Earth Pressure.

a. Superposition of Pressures. The distribution of total horizontal pressure on the driving or resisting side is obtained by superposing the distributions due to horizontal effective earth pressure, water, and surcharges. Where compaction efforts are specified, horizontal earth pressures should be calculated in accordance with paragraph 3-17.

b. Soils Completely Above or Completely Below the Water Table. The effective earth pressure may be assumed to have a triangular distribution when all of the following conditions hold:

(1) The wall will not move or it will rotate about the base.

(2) The water table is at or below the base of the wall or at or above the top of the wall (submerged soil).

(3) Water conditions are hydrostatic (no seepage).

(4) There is only one soil material.

(5) There is no cohesion (c = 0).

(6) The backfill surface is plane (it may be inclined).

The distribution is given by:

$$p'_{hz} = K\gamma' z \qquad [3\text{-}39]$$

where

$K = K_o$ on the driving side. K for the resisting side could vary between K_p and K_o or could be taken as zero

γ' = the effective unit weight (total, saturated or moist unit weight if above the water table, buoyant or submerged unit weight if below the water table)

z = vertical distance measured down from the backfill surface

See Figure 3-19 for an example.

c. Partly Submerged Soils. Where the water table occurs between the top and the base of the wall, and only one soil is present, the top portion of the pressure diagram is a triangle given by Equation 3-39 and the bottom is a trapezoid given by:

$$p'_{hz} = K[\gamma z_w + \gamma' (z - z_w)] \qquad [3\text{-}40]$$

where

z_w = depth to water table

$\gamma' = (\gamma - \gamma_w)$ below the water table

An example is shown in Figure 3-20. See Appendix H where water table and backfill surface are not parallel.

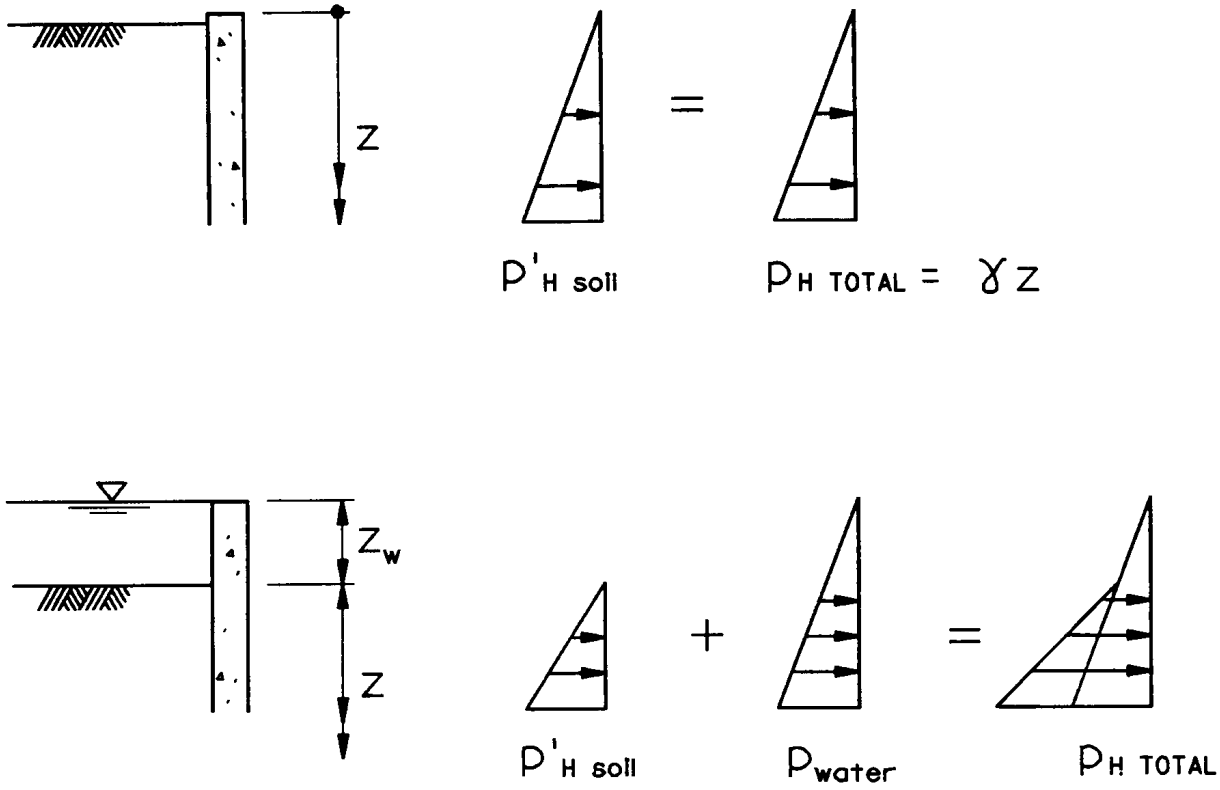

$$P_v = P_v + P_{water}$$
$$= \gamma_w z_w + \gamma z$$
$$P'_v = P_v - P_{water}$$
$$= \gamma_w z_w + \gamma z - \gamma_w (z_w + z)$$
$$= (\gamma - \gamma_w) z$$
$$= \gamma' z$$
$$P'_H = K \gamma' z$$

Figure 3-19. Lateral pressures, one soil completely above water table or completely below water table

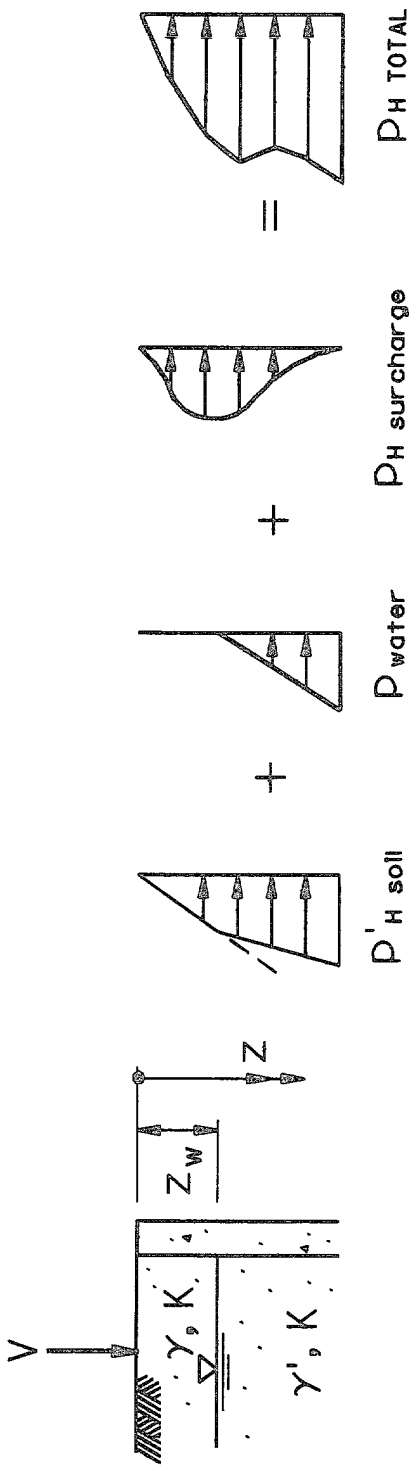

Figure 3-20 Lateral pressures, one soil, water, finite surcharge

d. Layered Soils. Where layered soils are present, the pressure diagram is a triangle underlain by a series of trapezoids given by:

$$p'_{hz} = K_i(p'_{vi} + \gamma'_i z_i) \qquad [3\text{-}41]$$

where

K_i = horizontal earth pressure coefficient for the i^{th} layer

p'_{vi} = vertical effective earth pressure at the top of the i^{th} layer

γ'_i = effective unit weight of the i^{th} layer

z_i = vertical distance measured down from the top of the i^{th} layer

An example is shown in Figure 3-21.

e. Irregular Backfills. Where the backfill is irregular, the pressure diagram may be estimated by performing successive wedge analyses at incremental depths from the top of the wall and applying the force difference from successive analyses over the corresponding vertical area increment (Agostinelli et al. 1981). Since this procedure is approximate, increasing the number of calculation points does not necessarily increase accuracy. An example of this procedure is shown in Figure 3-22. The pressure diagram may also be estimated by the use of pressure coefficients (see paragraphs 3-13c(6)) as shown in examples 7, 8, and 9 of Appendix M.

f. Cohesion Effects.

(1) Where the backfill is horizontal and where cohesion is present, its theoretical effect is to reduce the driving side earth pressure by $2c\sqrt{K_A}$ for the entire depth of the soil layer (see Equation 3-18). This infers tension in the soil to a "crack depth" d_c where

$$d_c = \frac{2c_d}{\gamma'\sqrt{K_A}} \qquad [3\text{-}42]$$

Consequently there is zero load on the wall in this region. For sloping backfills, see Appendixes H and I. Where cohesion is present, a water-filled tension crack should be considered in the inferred tension zone. The maximum crack depth using the unfactored c value should also be checked. Where the horizontal earth force is calculated from a pressure diagram that includes negative pressure, the force reduction due to the inferred negative pressure zone should be taken as zero. The pressure on the driving side should be

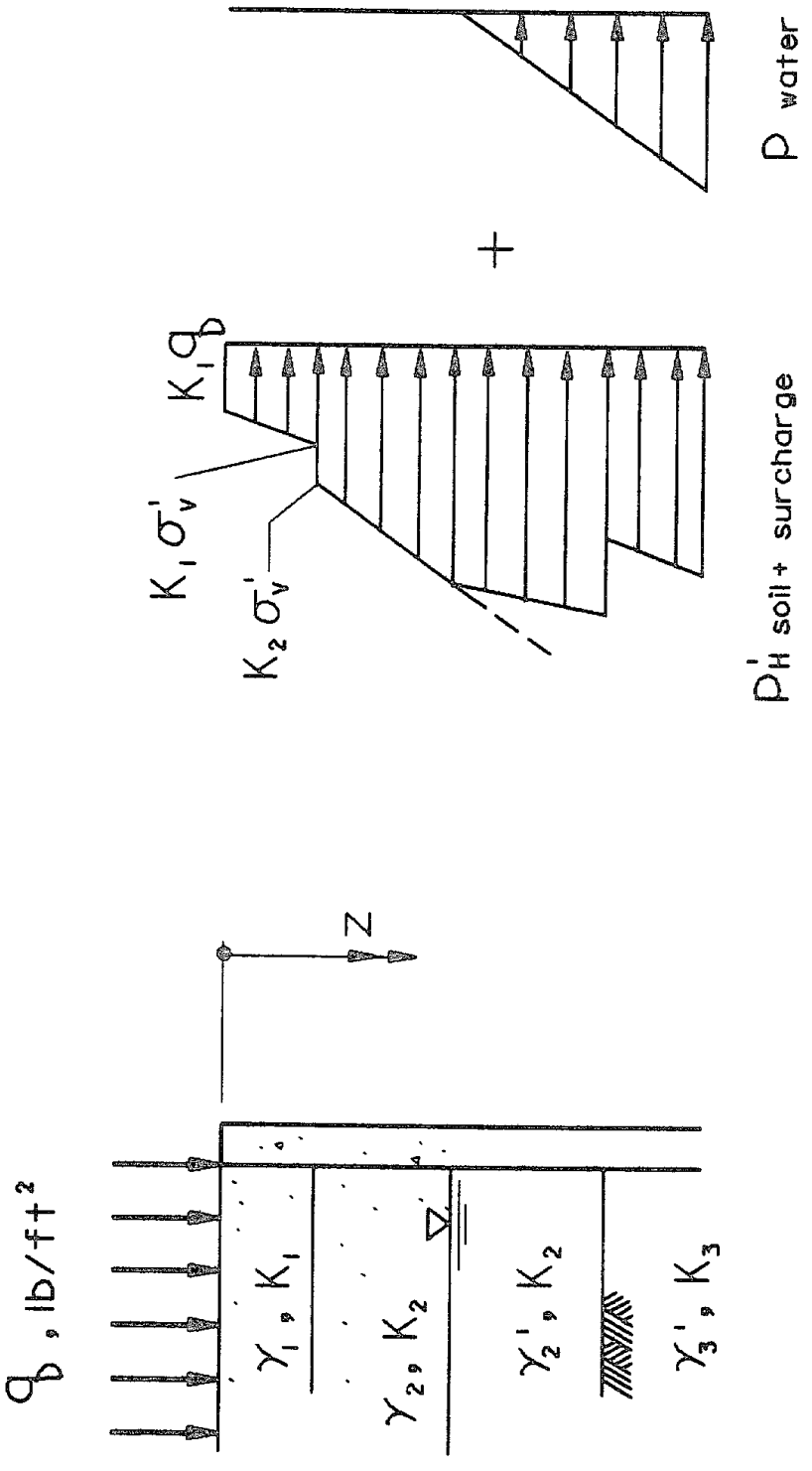

Figure 3-21. Lateral pressures, three soils, water

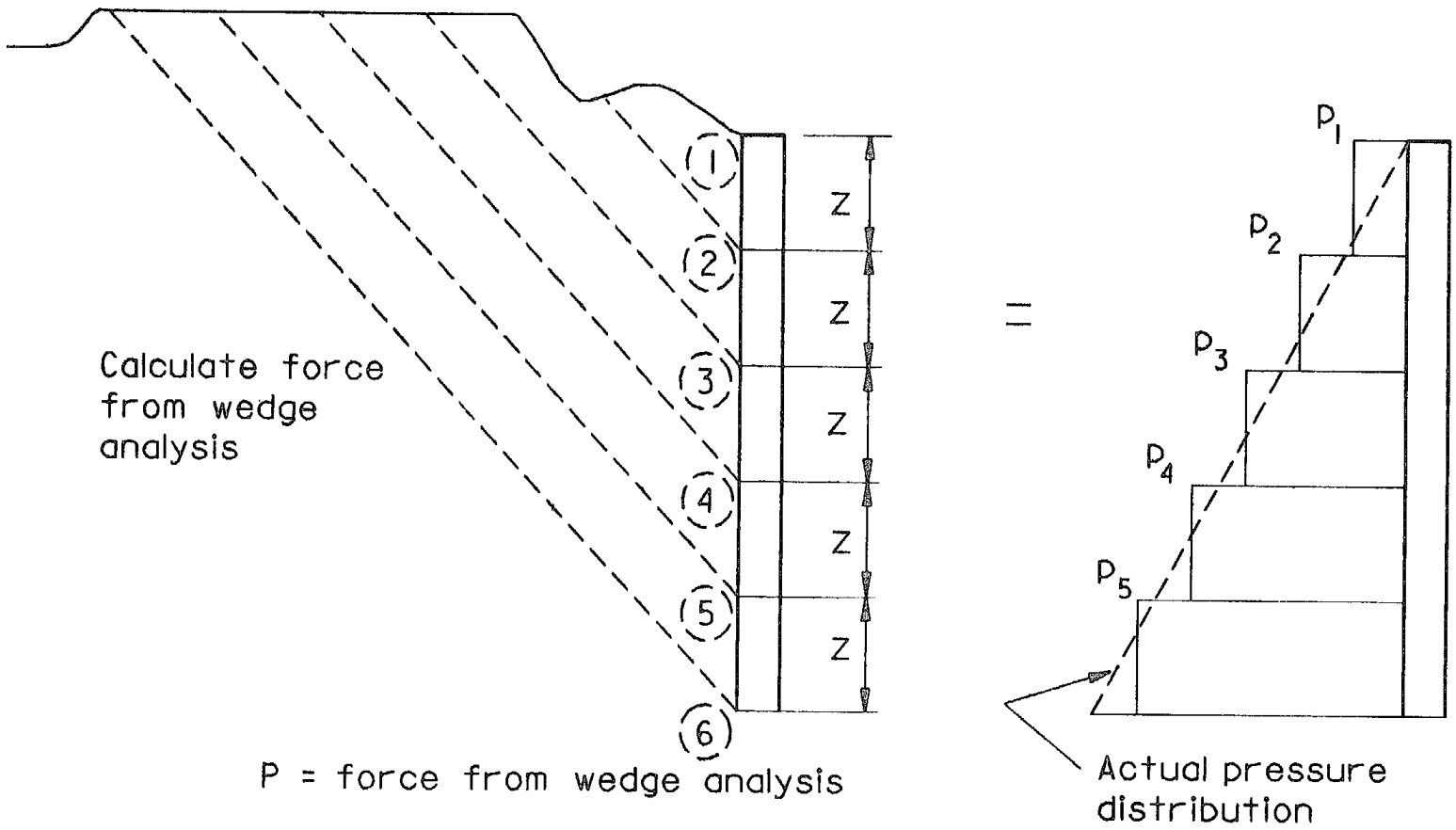

P = force from wedge analysis

$$P_1 = \frac{P_2 - P_1}{Z} \quad ,$$

$$P_2 = \frac{P_3 - P_2}{Z} \quad , \quad \text{etc....}$$

Figure 3-22. Pressure distribution due to irregular backfill

computed using Equation 3-18 by setting the 2nd term equal to 0 and K_A equal to K_o and using the pressure distribution as shown in Figure 3-23.

(2) For the resisting side, passive pressure theory indicates no tension crack will form and the pressure would be calculated using Equation 3-22. The pressure distribution for a cohesive soil on the resisting side of a structure is shown in Figure 3-24. However, for operating conditions without movement, a tension crack may form due to moisture loss reducing or eliminating the resisting side pressure. See paragraph 3-8 for resisting pressure to be used for design.

(3) Refer to guidance on use of cohesive materials in paragraph 3-5.

g. Wall Movement Effects.

(1) Where the expected mode of wall movement is translation and/or rotation about a point other than the base (such as for braced walls) the value of K varies with depth and the horizontal earth pressure distribution will be parabolic rather than triangular. Solution methods for such conditions are less reliable than those for rotation about the base. Available methods include Rendulic's procedure (Winterkorn and Fang 1975), Dubrova's procedure (Harr 1977), and a procedure given by Wu (1966).

(2) Where the expected mode of wall movement is translation and/or rotation about a point other than the base, the force may be assumed the same as that obtained for rotation about the base, but the point of application should be taken at 45 percent of the wall height above the base.

3-16. Surcharge Effects.

a. Uniform Surcharges. Where uniform surcharges (q) are present, the vertical effective stress increases by the amount of the surcharge and the horizontal earth pressure diagram is a trapezoid given by:

$$p'_{hz} = K(q + \gamma' z) \qquad [3\text{-}43]$$

An example is shown in Figure 3-21.

b. Finite Surcharges.

(1) Pressure Increase Due to Finite Surcharges. The distribution of the horizontal pressure increase due to finite surcharges should be calculated using experimentally modified elastic theory where expected (or allowable) strains due to the surcharge are small. Pressures due to point and line loads can be calculated using Figures 3-25 and 3-26, respectively. The resulting pressures are about twice as great as would be obtained from either unadjusted elastic solutions or limit-equilibrium solutions. This difference is due to wall rigidity not considered in elastic or limit-equilibrium methods. Pressures due to strip loads can be calculated using Figure 3-27. Pressures due

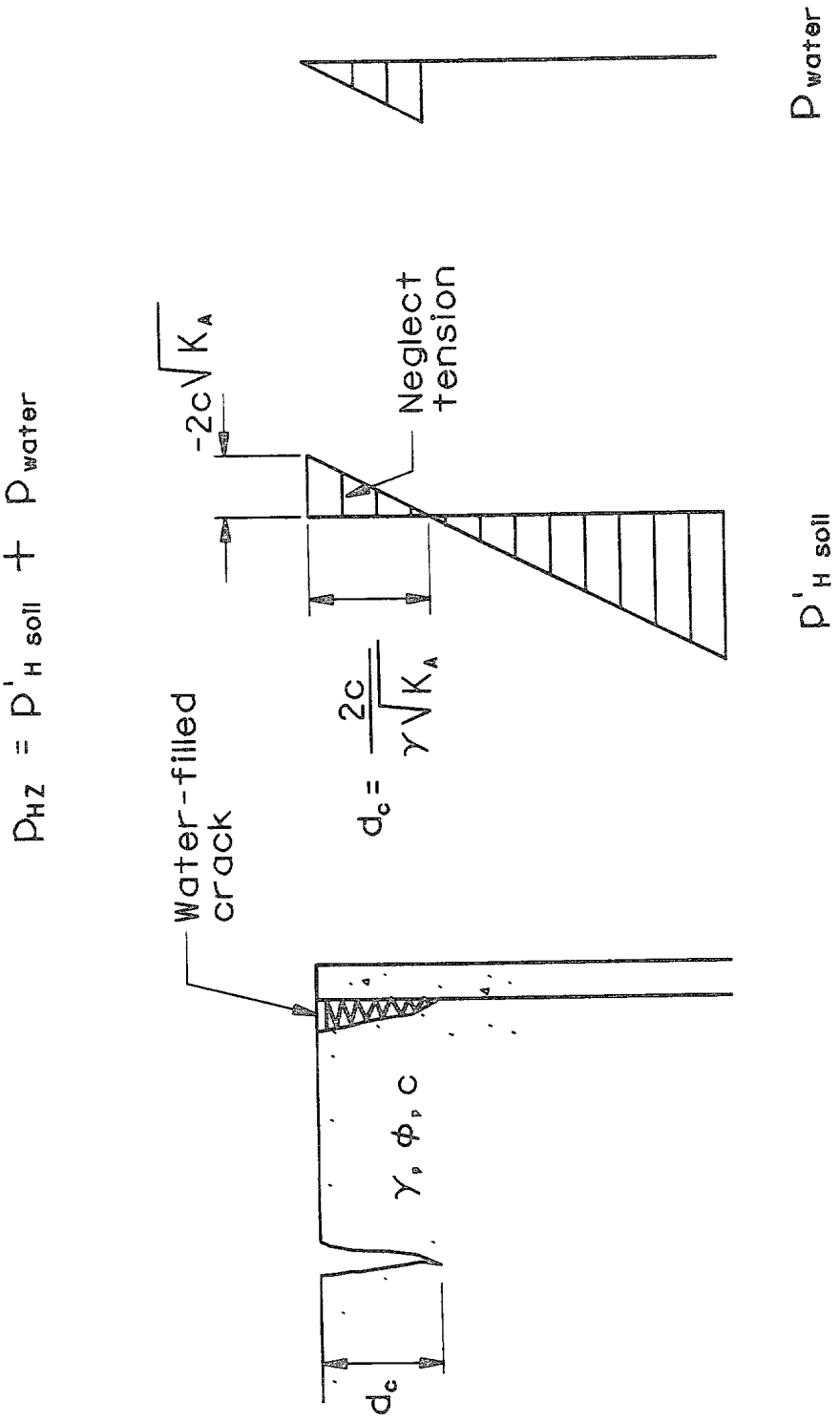

Figure 3-23. Lateral pressure distribution; active case, soil with cohesion

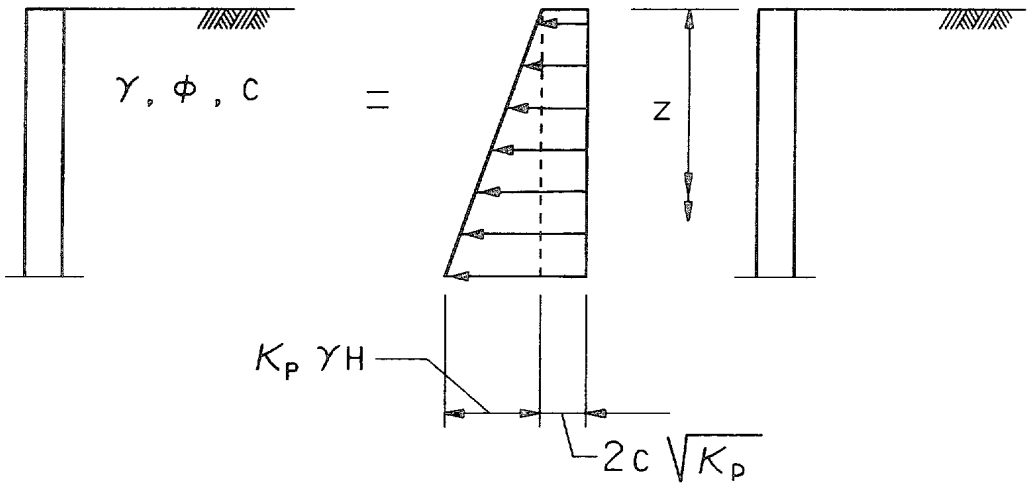

$$P_{PH} = K_P \gamma' z + 2c\sqrt{K_P}$$

Figure 3-24. Lateral pressure distribution; passive case, soil with cohesion

to strip surcharge loads of more general shapes can be calculated by applying the principle of superposition to these solutions; a pressure-intensity curve of any shape can be modeled to any desired degree of accuracy as the sum of point, line, or strip loads. Example computations involving surcharges are shown in examples 4 and 10 of Appendix M.

(2) Force Due to Finite Surcharges. Point, line, or nonuniform (finite) surcharge loads are supported by distribution or "diffusion" of stresses within the backfill material. These result in a curved pressure diagram; the point of application for the horizontal force resultant due to point or line loads is given in Figure 3-28. Where surcharge pressure distributions of a general shape have been modeled by superposition of these basic solutions, the point of application is found by dividing the total moment due to the surcharge resultants by the sum of the surcharge resultants. Where surcharge loadings are included in a wedge-method analysis, the difference in resultant force due to the surcharge (ΔP_H) should be applied at a different point on the wall from the resultant due to backfill weight. An approximate method for locating the line of action for a line load (Terzaghi 1943) is shown in Figure 3-29. An example using this approximate method is shown in example 4 of Appendix M.

3-17. Earth Pressures Due to Compaction. The use of heavy rollers for compaction adjacent to walls can induce high residual pressures against the wall. Although a reasonable degree of compaction is necessary to provide adequate shear strength and minimize settlement, excess backfill compaction should be avoided. Ingold (1979a,b) proposed a procedure for estimating lateral pressures due to compaction that has been modified herein (Appendix J) to account

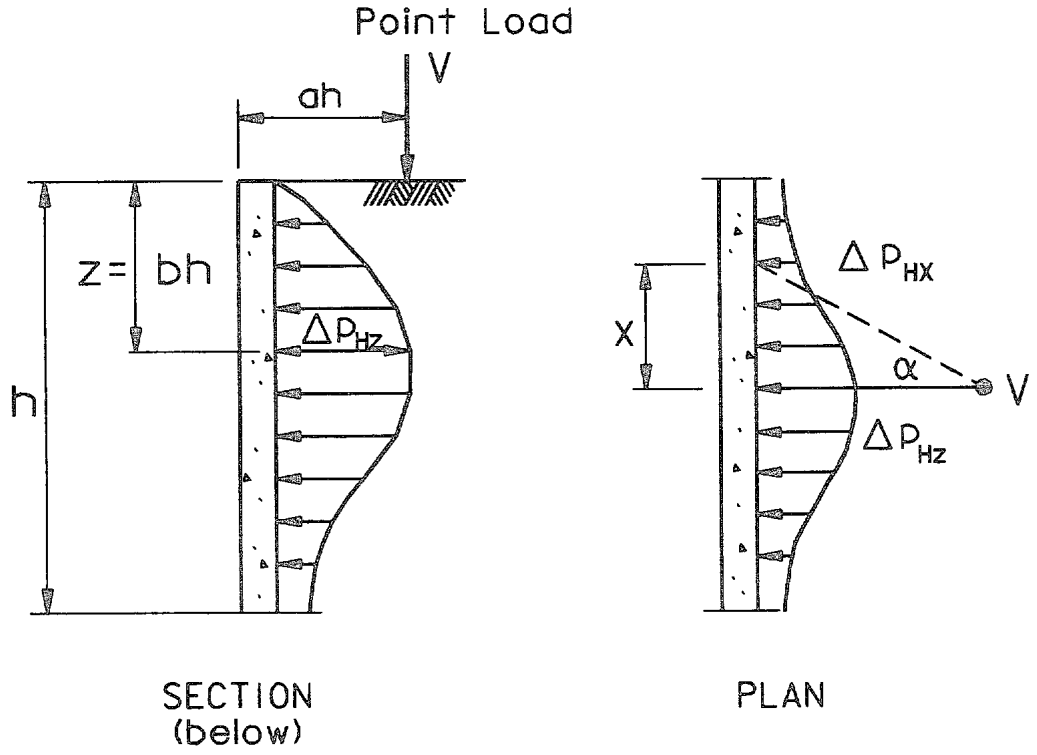

Increase in horizontal pressure, ΔP_{Hz}, on a section through point load, V

$$\Delta P_{Hz} = \left(\frac{V}{h^2}\right)\left(\frac{a^2 b^2}{(a^2 + b^2)^3}\right) \quad \text{for } a > 0.4$$

$$\Delta P_{Hz} = \left(\frac{0.28V}{h^2}\right)\left(\frac{b^2}{(0.16 + b^2)^3}\right) \quad \text{for } a \leq 0.4$$

Increase in horizontal pressure, ΔP_{HX}, at distance X from plane of load, V

$$\alpha = \tan^{-1}\left(\frac{X}{ah}\right)$$

$$\Delta P_{HX} = \Delta P_{Hz} \cos^2(1.1\alpha)$$

Figure 3-25. Increase in pressure due to point load (after Spangler 1956)

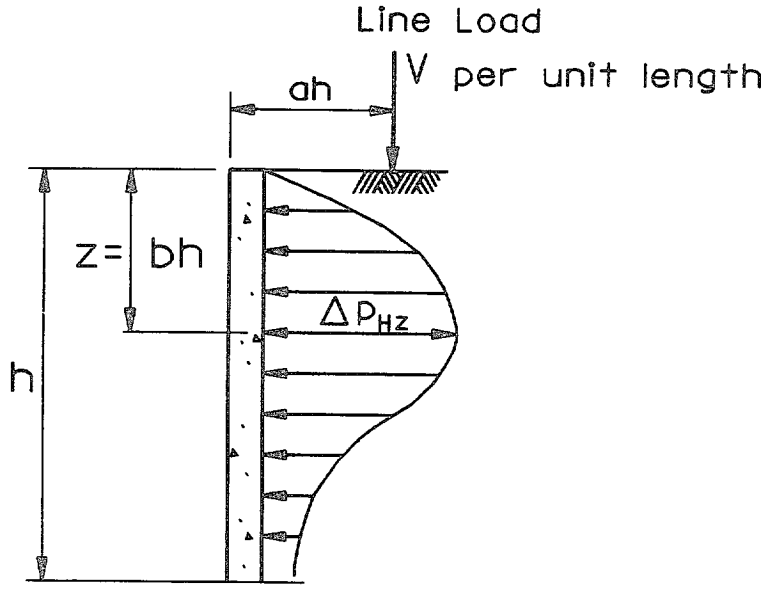

Increase in horizontal pressure, ΔP_{Hz}, at depth bH due to line load, V/ft at distance aH from wall.

$$\Delta P_{Hz} = \left(\frac{4V}{\pi h}\right)\left(\frac{a^2 b}{(a^2 + b^2)^2}\right) \quad \text{for } a > 0.4$$

$$\Delta P_{Hz} = \left(\frac{V}{h}\right)\left(\frac{0.203\, b}{(0.16 + b^2)^2}\right) \quad \text{for } a \leq 0.4$$

Figure 3-26. Increase in pressure due to line load (after Spangler 1956)

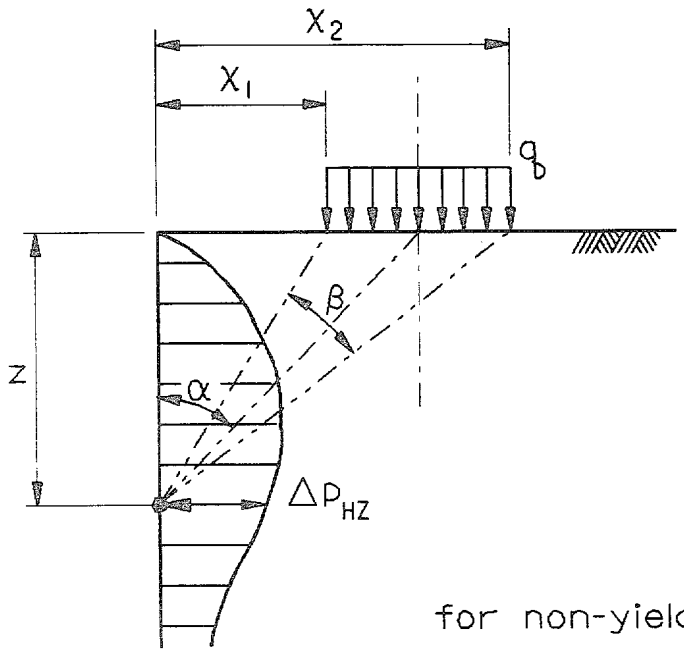

$$q_b = \frac{V}{(X_2 - X_1)}$$

for non-yielding walls:

$$\Delta P_{HZ} = \frac{2 q_b}{\pi} \left(\beta - \sin\beta \cos 2\alpha\right)$$

for yielding walls,
(walls at failure):

$$\Delta P_{HZ} = \frac{q_b}{\pi} \left(\beta - \sin\beta \cos 2\alpha\right)$$

β in radians

$$\beta = \tan^{-1}\left(\frac{X_2}{z}\right) - \tan^{-1}\left(\frac{X_1}{z}\right)$$

$$\alpha = \tan^{-1}\left(\frac{X_2 + X_1}{2z}\right)$$

Figure 3-27. Increase in pressure due to strip load

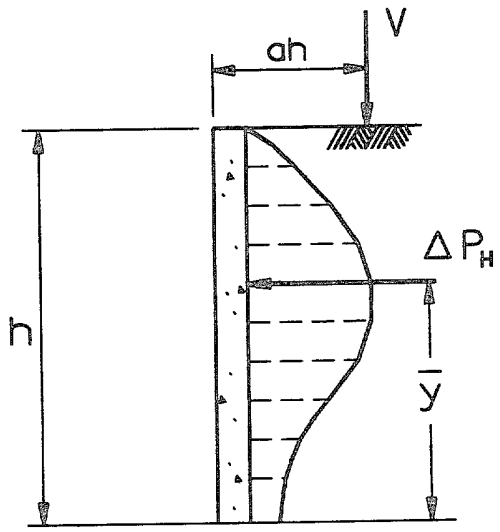

Point Load, V

a	ΔP_H	$\bar{y}$
0.4	0.78 (V/h)	.59 h
0.5	0.60 (V/h)	.54 h
0.6	0.46 (V/h)	.48 h

Line Load, V/ft

for $a \leq 0.4$ $\quad \Delta P_H = 0.55\ V$

for $a > 0.4$ $\quad \Delta P_H = \dfrac{0.64\ V}{(a^2 + 1)}$

a	$\bar{y}$
0.4	0.60 h
0.5	0.56 h
0.6	0.52 h
0.7	0.48 h

Figure 3-28. Resultant forces, point and line loads (after Spangler 1956)

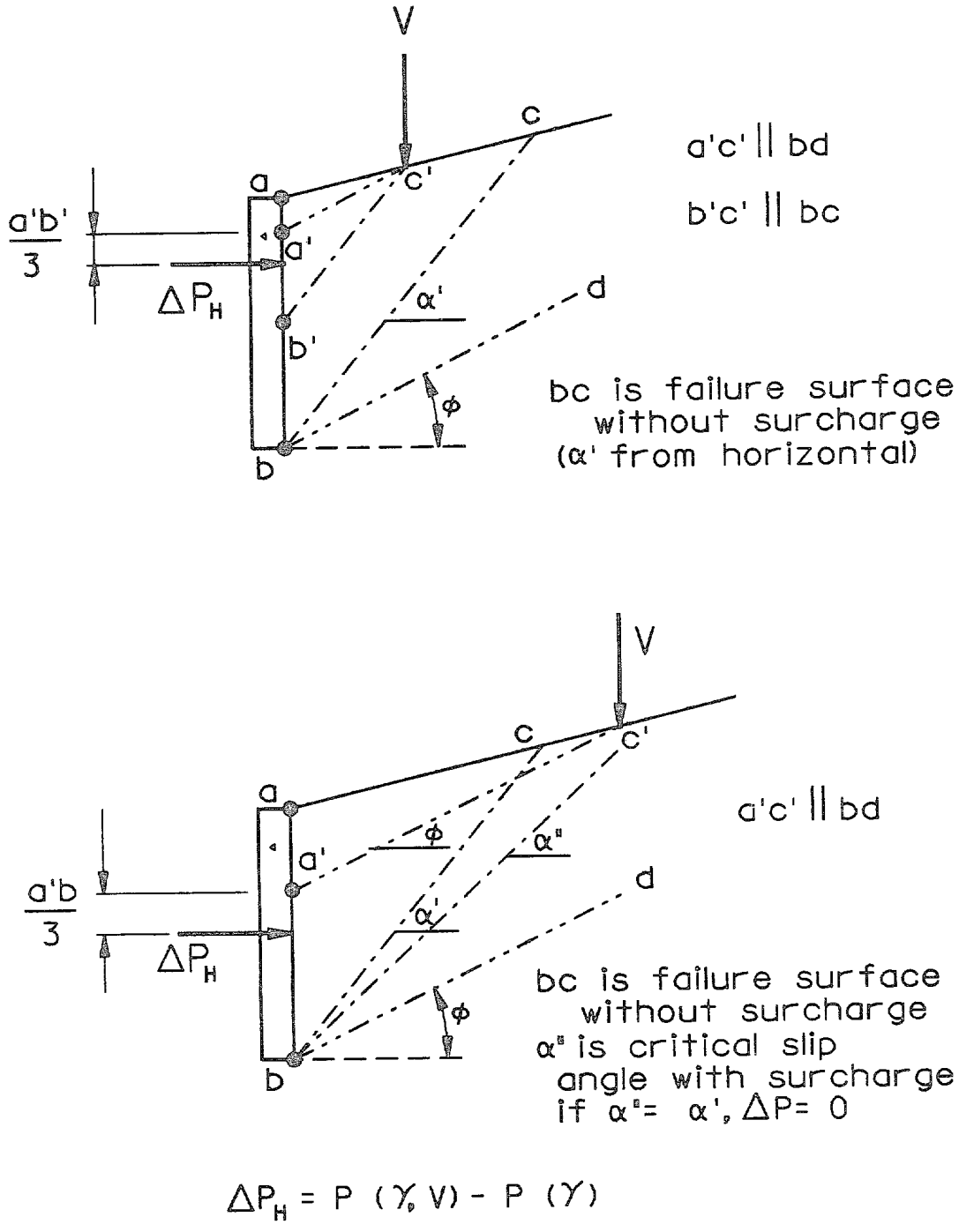

$$\Delta P_H = P(\gamma, V) - P(\gamma)$$

Figure 3-29. Approximate line of action for line loads (Terzaghi 1943)

for walls designed for at-rest conditions. The roller is assumed to exert a line load of P lb/ft obtained from the roller weight and drum dimensions; double this value is recommended for vibratory rollers. The design pressure diagram (Figure 3-30) is composed of three linear segments:

a. Starting at the top of the wall, the pressure increases linearly to a value of p'_{hm} at a depth z_{cr}. In this region, the horizontal stress is increased during compaction due to the roller pressure but then the horizontal stress is reduced by passive failure when the roller is removed.

b. The horizontal pressure is constant with depth from z_{cr} to z_2 and is compaction induced.

c. At depth z_2, the compaction-induced pressure equals the horizontal pressure due to soil weight (at-rest pressure). The pressure increases linearly below this depth according to the equations in paragraph 3-15.

Compaction-induced pressures need only be considered for structural design. For overturning, bearing, and sliding analyses, any wall movement due to compaction-induced pressures would be accompanied by a reduction in the pressure. As shown by the calculations in Appendix J, horizontal pressures due to compaction may exceed the at-rest pressure in only the upper few feet unless roller loads are particularly high. The effects of compaction are shown in example 1 of Appendix M.

Section III. Water Pressures

3-18. Pressure Calculations. In all cases, water pressures at a point may be calculated by multiplying the pressure head at the point by the unit weight of water (62.4 lb/cu ft). As water has no shear strength, water pressures are equal in all directions (K = 1.0). The pressure head is equal to the total head minus the elevation head. The pressure head at a point is the height water would rise in a piezometer placed at the point. The elevation head is the height of the point itself above an arbitrary datum. Water pressures must be added to effective earth pressures to obtain total pressures.

a. Static Pressures. For static water (no seepage) above or below the ground surface, the total head is constant and the pressure head at any point is the difference in elevation between the water surface and the point.

b. Water Pressures with Earth Pressure Equations. Where Coulomb or at-rest equations are used to calculate the driving-side earth pressures for a totally submerged soil mass, the buoyant soil weight ($\gamma' = \gamma_{sat} - \gamma_w$) is used in the earth pressure equations and the calculated effective earth pressures are added to the calculated water pressures.

c. Water Forces with Wedge Analysis. The wedge method (Equations 3-23 and 3-33) uses total densities, uplift forces, and horizontal water forces on

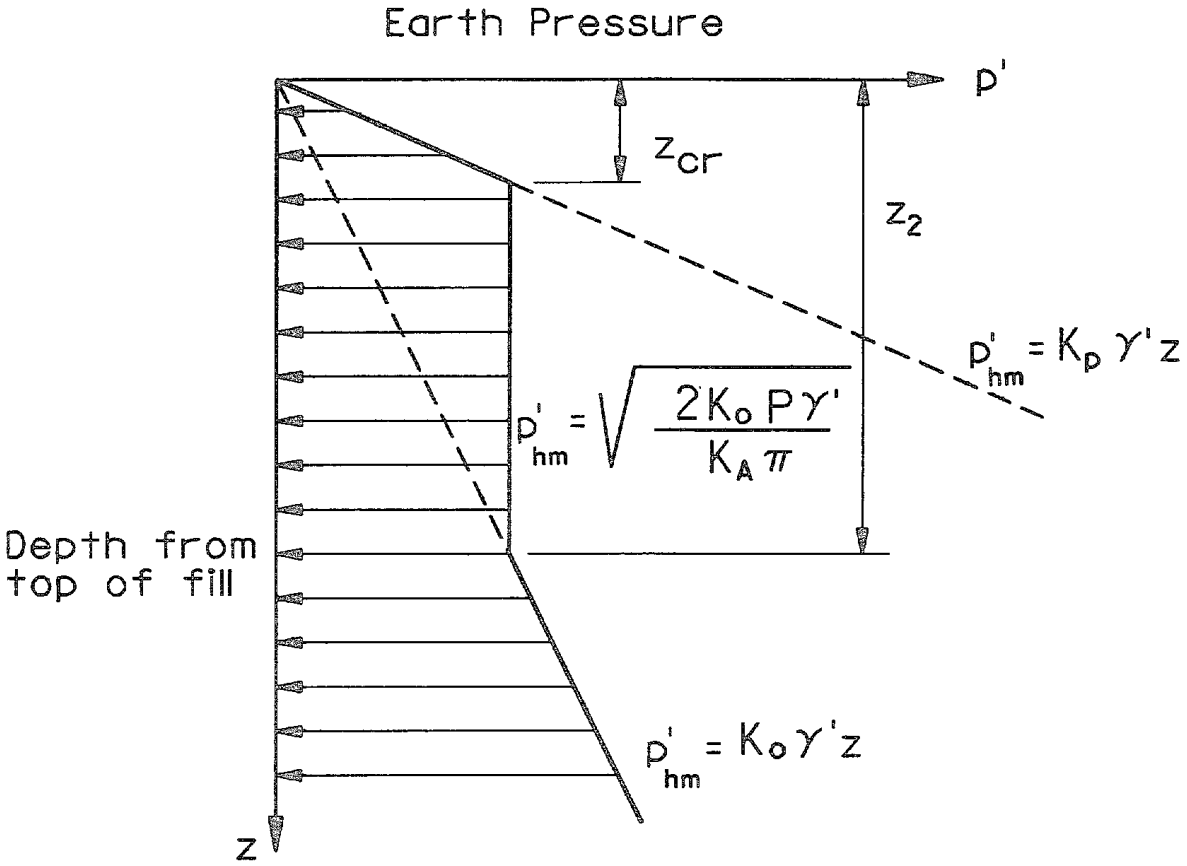

$$z_{cr} = \sqrt{\frac{2K_A K_o P}{\pi \gamma'}} \qquad z_2 = \sqrt{\frac{2P}{K_A K_o \pi \gamma'}}$$

P is roller line load, lb/ft (use twice roller weight for vibratory rollers)

Figure 3-30. Design pressure envelope for nonyielding walls with compaction effects

the vertical sides of the wedge. Consequently, it gives the effective earth force, and water forces must be added to obtain total forces (see example 3 in Appendix M).

d. Water Pressures Where Seepage is Present. Where seepage occurs, the pressure head at points of interest must be obtained from a seepage analysis. Such an analysis must consider the types of foundation and backfill materials, their possible range of horizontal and vertical permeabilities, and the effectiveness of drains. Techniques of seepage analysis are discussed in EM 1110-2-1901, Casagrande (1937), Cedergren (1967), Harr (1962), and other references. Techniques applicable to wall design include flow nets and numerical methods such as the finite element method and the method of fragments. An example of pressure calculations using a flow net is shown in Figure 3-31. Where soil conditions adjacent to and below a wall can be assumed homogeneous (or can be mathematically transformed into equivalent homogeneous conditions) simplified methods such as the line-of-creep method may be used. Simplified methods are advantageous for preliminary studies to size wall elements or compare alternate wall designs; however, designers should ensure that the final design incorporates water pressures based on appropriate consideration of actual soil conditions.

3-19. Seepage Analysis by Line-of-Creep Method. Where soil conditions can be assumed homogeneous, the line-of-creep (or line-of-seepage) method provides a reasonable approximate method for estimating uplift pressures that is particularly useful for preliminary or comparative designs. The line of creep may underestimate uplift pressures on the base and thus be unconservative. Therefore, final design should be based on a more rigorous analysis. The method is illustrated in Figure 3-32. The total heads at the ends of the base (points B and C) are estimated by assuming that the total head varies linearly along the shortest possible seepage path (A'BCD'). Once the total head at B and C is known, the uplift pressures U_B and U_C are calculated by subtracting the elevation head from the total head at each point and multiplying the resulting pressure head by the unit weight of water. The total uplift diagram along the failure surface is completed in a similar manner. Where a key is present (Figure 3-33), point B is at the bottom of the key and line segment BC is drawn diagonally. Examples using the line-of-creep method are contained in Appendix N.

3-20. Seepage Analysis by Method of Fragments. Another approximate method applicable to homogeneous soil conditions is the method of fragments. It is more accurate than the line-of-creep method. The soil is divided into a number of regions or fragments for which exact solutions of the seepage conditions exist. The head loss through each fragment is calculated by mathematically combining the assemblage of fragments. The method assumes that fragment boundaries are equipotential lines (contours of equal total head) and provides an exact solution where this assumption is true (I-walls and single sheet piles). Details of the method and instructions for the computer program CFRAG (Appendix O) are presented by Pace, et al. (1984). Further background on the method is presented by Harr (1962, 1977). Keyed bases should be modeled by treating the key as a sheet pile and the soil below the base as a

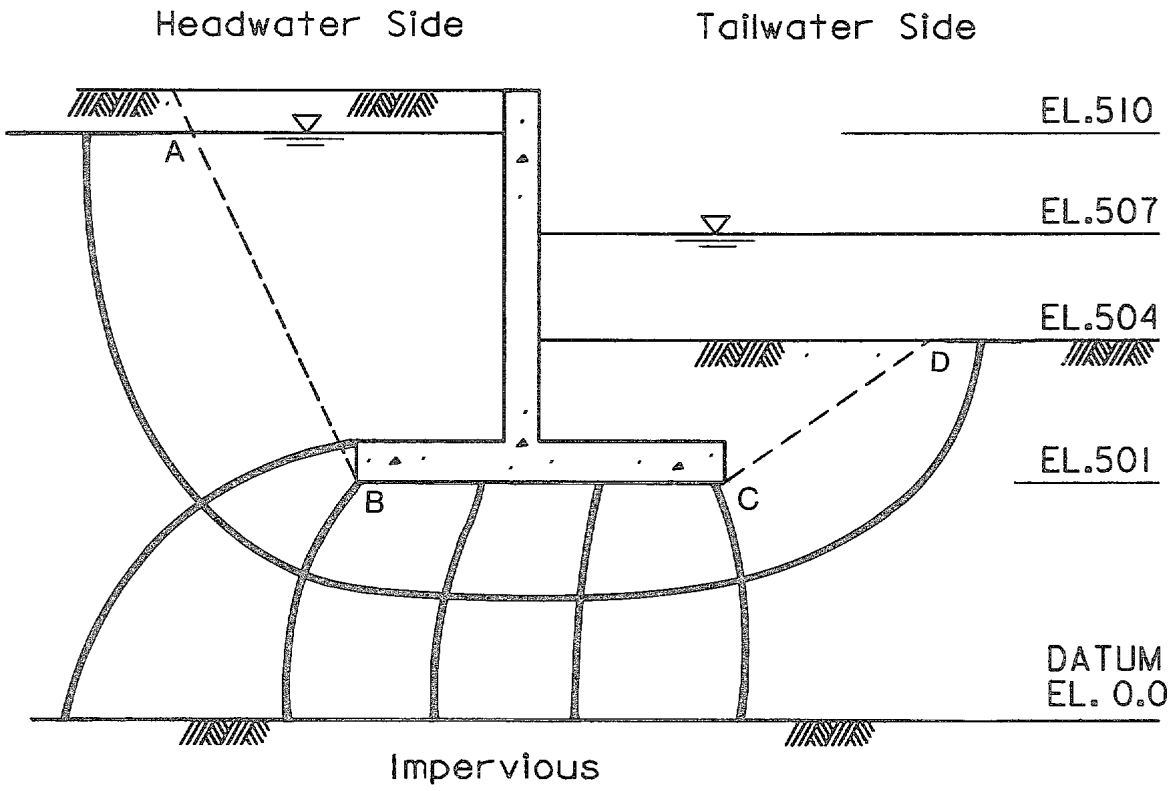

Pt. A Total Head: 510
Elevation Head: 510
Pressure Head: 0
Pressure: 0

Pt. B Total Head: $510 - (2/6)(510 - 507) = 509$
$507 + (4/6)(3) = 509$

Elevation Head: 501
Pressure Head: $509 - 501 = 8'$

Pressure: $(8)(62.4) = 499.2\ lb/ft^2$

Figure 3-31. Water pressures from flow net

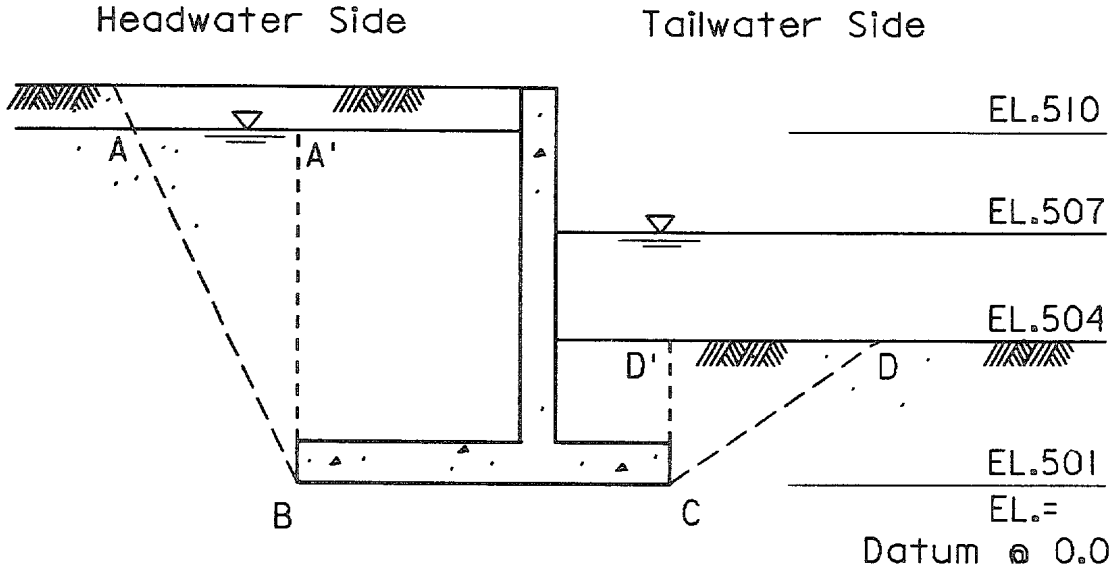

Length of Shortest Seepage Path: A'BCD'

(A') Total Head at A': 510 ft.
Elevation Head at A': 510 ft.
Pressure Head at A': 0 ft.

(B) Total Head at B: $510 - \left[\frac{(A'B)}{(A'BCD')}\right](510 - 507)$

Elevation Head at B: 501
Pressure Head at B = Total Head - Elevation Head

(C) Total Head at C: $510 - \left[\frac{(A'BC)}{(A'BCD')}\right](510 - 507)$

Elevation Head at C: 501

etc.

Water Pressure: $P_w = \gamma_w \cdot (\text{Pressure Head})$

Figure 3-32. Water pressure by line-of-creep method

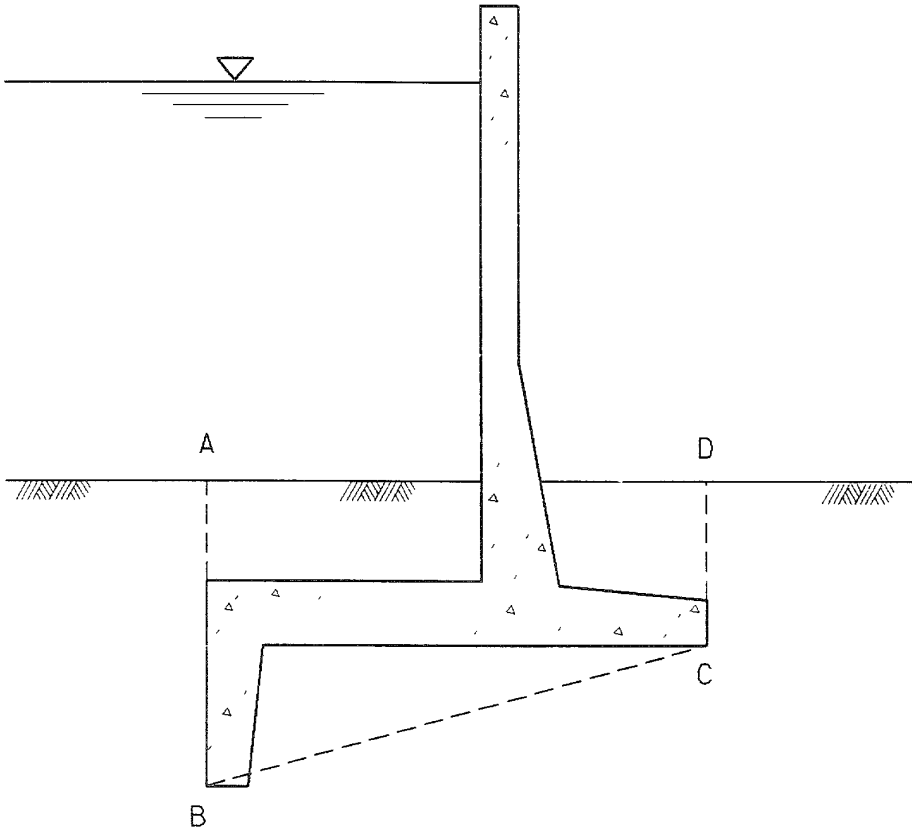

Figure 3-33. Seepage path for line of creep

type IV. Accuracy is improved by minimizing the number of fragments, not by maximizing them to incorporate minor changes in geometry. Where water pressure on the base of a wall is calculated by the method of fragments, the water pressure along the driving-side and resisting-side wedge bases may be taken to vary linearly as described in the preceding paragraph.

3-21. Seepage Analysis by the Finite Element Method. The finite element method provides a powerful tool to solve confined or unconfined seepage problems involving multiple soils with isotropic or anisotropic permeabilities. It is particularly useful for evaluating the effect of drains and analyzing walls with complicated foundation and backfill geometry. The WES computer program for the finite element method is described by Tracy (1983). Pre- and post-processors for the program are also available (Tracy 1977a, 1977b).

3-22. Uplift Calculations for Rock Foundations. Seepage beneath flood walls

founded on competent rock typically occurs in joints and fractures, not uniformly through pores as assumed for soils. Consequently, the assumptions of isotropy and homogeneity and the use of two-dimensional analysis models commonly employed for soil foundations will generally be invalid. Total head, uplift pressure, and seepage quantities may be highly dependent on the type, size, orientation, and continuity of joints and fractures in the rock and the type and degree of treatment afforded the rock foundation during construction. Since any joints or fractures in the rock can be detrimental to underseepage control, the joints and fractures should be cleaned out and filled with grout before the concrete is placed, as discussed in paragraph 7-4g. For walls on a rock foundation, the total seepage path can be assumed to be the length of the base which is in compression. An example of a wall on a rock foundation is shown in example 2 of Appendix N.

3-23. Effect of Drains. Water pressures for design analyses should consider both working drains and blocked drainage conditions. Achieving an adequate factor of safety for an analysis considering blocked drainage is usually not good justification for omitting drains. Preferred practice is to provide drains; lower factors of safety than specified herein may be justified where blocked drainage assumptions are combined with rare and/or conservative loading assumptions. All such deviations from recommended safety factors should be supported by an assessment of expected drain reliability, and a justification that the factor of safety is reasonable in light of the analyzed conditions. Drains are discussed further in paragraphs 6-6 and 7-4.

3-24. Surge and Wave Loads.

a. General Criteria. Wave and water level predictions for the analysis of walls should be determined with the criteria presented in the Shore Protection Manual (U. S. Army Engineer Waterways Experiment Station 1984). Design forces acting on the wall should be determined for the water levels and waves predicted for the most severe fetch and the effects of shoaling, refraction, and diffraction. A distinction is made between the action of nonbreaking, breaking, and broken waves, where the methods recommended for calculation of wave forces are for vertical walls. Wave forces on other types of walls (i.e., sloping, stepped, curved, etc.) are not sufficiently understood to recommend general analytical design criteria. In any event, a coastal engineer should be involved in establishing wave forces for the design of important structures.

b. Wave Heights. Wave heights for design are obtained from the statistical distribution of all waves in a wave train, and are defined as follows:

H_s = average of the highest one-third of all waves

$H_1 = 1.67\ H_s$ = average of highest 1 percent of all waves

H_b = height of wave which breaks in water depth d_b

c. Nonbreaking Wave Condition. When the depth of water is such that

waves do not break, a nonbreaking condition exists. This occurs when the water depth at the wall is greater than approximately 1.5 times the maximum wave height. The H_1 wave shall be used for the nonbreaking condition. Design nonbreaking wave pressures shall be computed using the Miche-Rudgren Method, as described in Chapter 7 of the Shore Protection Manual (U. S. Army Engineer Waterways Experiment Station 1984). Whenever the maximum stillwater level results in a nonbreaking condition, lower stillwater levels should be investigated for the possibility that shallow water may produce breaking wave forces which are larger than the nonbreaking forces.

d. Breaking Wave Condition. The breaking condition occurs when the steepness of the wave and the bottom slope on the front of the wall have certain relationships to each other. It is commonly assumed that a structure positioned in a water depth d_s will be subject to the breaking wave condition if $d_s \leq 1.3\ H$ where H is the design wave height. Study of the breaking process indicates that this assumption is not always valid. The height of the breaking wave and its breaking point are difficult to determine, but breaker height can be equal to the water depth of the structure, depending on bottom slope and wave period. Detailed determination of breaker heights and distances for a sloping approach grade in front of the wall are given in the Shore Protection Manual (U. S. Army Engineer Waterways Experiment Station 1984). Special consideration must be given to a situation where the fetch shoals abruptly (as with a bulkhead wall submerged by a surge tide) near the wall, but at a distance more than an approximate 0.7 wavelength away from the wall, and then maintains a constant water depth from that point to the wall. In this case waves larger than the water depth can be expected to have broken at the abrupt shoaling point, leaving smaller, higher frequency waves to reach the wall. Design breaking wave pressure should be determined by the Minikin method presented in Chapter 7 of the Shore Protection Manual (U. S. Army Engineer Waterways Experiment Station 1984). Breaking wave impact pressures occur at the instant the vertical force of the wave hits the wall and only when a plunging wave entraps a cushion of air against the wall. Because of this dependence on curve geometry, high impact pressures are infrequent against prototype structures; however, they must be recognized and considered in design. Also, since the high impact pressures caused by breaking waves are of high frequency, their importance in design against sliding and overturning may be questionable relative to longer lasting lower dynamic forces. An example involving a breaking wave condition is shown in example 7 of Appendix N.

e. Broken Wave Condition. Broken waves are those that break before reaching the wall but near enough to have retained some of the forward momentum of breaking. The design breaker height in this case (H_b) is the highest wave that will be broken in the break zone. Design wave forces for the height H_b should be determined by the method presented in Chapter 7 of the Shore Protection Manual (U. S. Army Engineer Waterways Experiment Station 1984).

f. Seepage Pressures. Seepage pressures are based on the elevation of the surge stillwater level (paragraph 4-5).

Section IV. Supplemental Forces

3-25. Wind Load. Wind loads should be considered for retaining and flood walls during construction, prior to placing backfill. Wind loads can act any time in the life of a flood wall. In locations subjected to hurricanes, a wind load of 50 lb/sq ft can be used conservatively for walls 20 feet or less in height for winds up to 100 miles per hour (mph). In locations not subjected to hurricanes, 30 lb/sq ft can be used conservatively for the same height of wall and wind velocity conditions. For more severe conditions, the wind loads should be computed in accordance with ANSI A58.1 using a coefficient C_f equal to 1.2.

3-26. Earthquake Forces.

a. General. For retaining walls which are able to yield laterally during an earthquake, the calculation of increased earth pressures induced by earthquakes can be approximated by the Mononobe-Okabe pseudo-static approach outlined below. In addition, the inertial forces of the wall, plus that portion of the adjacent earth and/or water which is assumed to act with the wall, should be included.

b. Mononobe-Okabe Analysis. This analysis is an extension of the Coulomb sliding-wedge theory taking into account horizontal and vertical inertial forces acting on the soil. The analysis is described in detail by Seed and Whitman (1970) and Whitman and Liao (1985).

(1) Assumptions. The following assumptions are made by the Mononobe-Okabe analysis:

(a) The wall is free to yield sufficiently to enable full soil strength or active pressure conditions to be mobilized.

(b) The backfill is completely above or completely below the water table, unless the top surface is horizontal, in which case the backfill can be partially saturated.

(c) The backfill is cohesionless.

(d) The top surface is planar (not irregular or broken).

(e) Any surcharge is uniform and covers the entire surface of the soil wedge.

(f) Liquefaction is not a problem.

(2) Equations. Equilibrium considerations of the soil wedge on the driving and resisting sides lead to the following Mononobe-Okabe equations for computing the active and passive forces exerted by the soil on the wall when the soil mass is at the point of failure (total shear resistance mobilized) along the slip plane of the Mononobe-Okabe wedge shown in Figure 3-34:

For driving (active) wedges (Figure 3-34a),

$$P_{AE} = \frac{1}{2} K_{AE} \gamma (1 - k_v) h^2 \qquad [3\text{-}44]$$

$$K_{AE} = \frac{\cos^2 (\phi - \Psi - \theta)}{\cos \Psi \cos^2 \theta \cos (\Psi + \theta + \delta) \left[1 + \sqrt{\frac{\sin (\phi + \delta) \sin (\phi - \Psi - \beta)}{\cos (\beta - \theta) \cos (\Psi + \theta + \delta)}} \right]^2} \qquad [3\text{-}45]$$

For resisting (passive) wedges (Figure 3-34b),

$$P_{PE} = \frac{1}{2} K_{PE} \gamma (1 - k_v) h^2 \qquad [3\text{-}46]$$

$$K_{PE} = \frac{\cos^2 (\phi - \Psi + \theta)}{\cos \Psi \cos^2 \theta \cos (\Psi - \theta + \delta) \left[1 - \sqrt{\frac{\sin (\phi + \delta) \sin (\phi - \Psi + \beta)}{\cos (\beta - \theta) \cos (\Psi - \theta + \delta)}} \right]^2} \qquad [3\text{-}47]$$

P_{AE} and P_{PE} are the combined static and dynamic forces due to the driving and resisting wedges, respectively. The equations are subject to the same limitations that are applicable to Coulomb's equations. Definitions of terms are as follows:

γ = unit weight of soil

k_v = vertical acceleration in g's

h = height of wall

ϕ = internal friction angle of soil

$\Psi = \tan \left(\frac{k_h}{1 - k_v} \right)$ = seismic inertia angle

k_h = horizontal acceleration in g's

θ = inclination of wall with respect to vertical (this definition of θ is different from θ in Coulomb's equations)

δ = wall friction angle

β = inclination of soil surface (upward slopes away from the wall are positive)

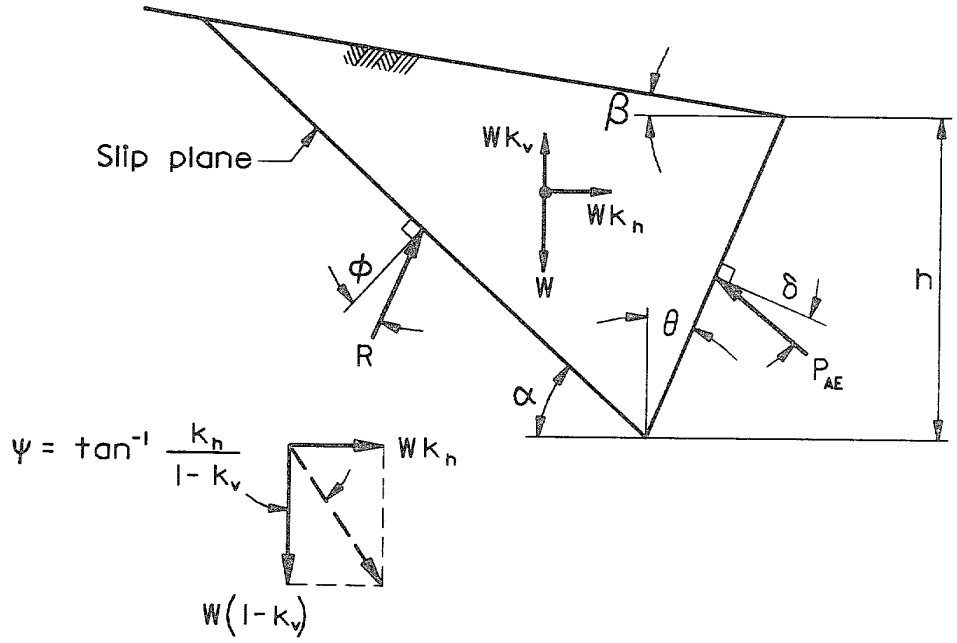

a. Mononobe-Okabe (active) wedge

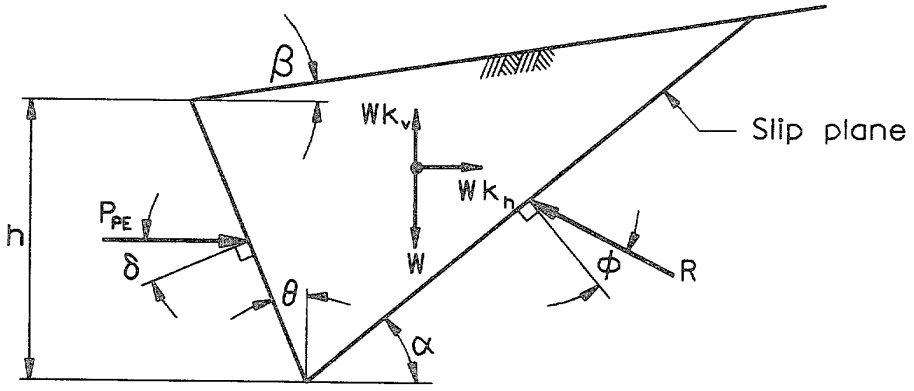

b. Passive wedge

Figure 3-34. Driving and resisting seismic wedges, no saturation

(3) Simplifying Conditions. For the usual case where k_v, δ, and θ are taken to be zero, the equations reduce to:

$$K_{AE} = \frac{\cos^2(\phi - \Psi)}{\cos^2 \Psi \left[1 + \sqrt{\frac{\sin \phi \sin(\phi - \Psi - \beta)}{\cos \beta \cos \Psi}}\right]^2} \quad [3\text{-}48]$$

$$K_{PE} = \frac{\cos^2(\phi - \Psi)}{\cos^2 \Psi \left[1 - \sqrt{\frac{\sin \phi \sin(\phi - \Psi + \beta)}{\cos \beta \cos \Psi}}\right]^2} \quad [3\text{-}49]$$

where

$$\Psi = \tan^{-1}(k_h)$$

and

$$P_{AE} = 1/2\, K_{AE} \gamma h^2$$

$$P_{PE} = 1/2\, K_{PE} \gamma h^2$$

For the case when the water table is above the backfill, P_{AE} and P_{PE} must be divided into static and dynamic components for computing the lateral forces. Buoyant soil weight is used for computing the static component below the water table, with the hydrostatic force added, and saturated soil weight is used for computing the dynamic component (see paragraph 3-26c(3)).

(4) Observations. General observations from using Mononobe-Okabe analysis are as follows:

(a) As the seismic inertia angle Ψ increases, the values of K_{AE} and K_{PE} approach each other and, for a vertical backfill face ($\theta = 0$), become equal when $\Psi = \phi$.

(b) The locations of P_{AE} and P_{PE} are not given by the Mononobe-Okabe analysis. Seed and Whitman (1970) suggest that the dynamic component ΔP_{AE} be placed at the upper one-third point, ΔP_{AE} being the difference between P_{AE} and the total active force from Coulomb's active wedge without the earthquake. The general wedge earthquake analysis described in paragraph 3-26c places the dynamic component ΔP_{AE} at the upper one-third point also, but computes ΔP_{AE} as being the difference between P_{AE} and the total active

force from the Mononobe-Okabe wedge. The latter method for computing ΔP_{AE}, which uses the same wedge for computing the static and dynamic components of P_{AE}, is preferred.

(c) Another limitation of the Mononobe-Okabe equation is that the contents of the radical in the equation must be positive for a real solution to be possible, and for this it is necessary that $\phi \geq \Psi + \beta$ for the driving wedges and $\phi \geq \Psi - \beta$ for the resisting wedges. This condition could also be thought of as specifying a limit to the horizontal acceleration coefficient that could be sustained by any structure in a given soil. The limiting condition for the driving wedge is:

$$k_h \leq (1 - k_v) \tan (\phi - \beta) \qquad [3\text{-}50]$$

and for the resisting wedge:

$$k_h \leq (1 - k_v) \tan (\phi + \beta) \qquad [3\text{-}51]$$

(d) Figure 3-35a (Applied Technology Council 1981) shows the effect on the magnification factor F_T (equal to K_{AE}/K_A) on changes in the vertical acceleration coefficient k_v. Positive values of k_v have a significant effect for values of k_v greater than 0.2. The effect is greater than 10 percent above and to the right of the dashed line. For values of k_h of 0.2 or less, k_v can be neglected for all practical purposes.

(e) K_{AE} and F_T are also sensitive to variations in backfill slope, particularly for higher values of horizontal acceleration. This effect is shown in Figure 3-35b.

c. General Wedge Earthquake Analysis. When the Coulomb wedge assumptions cannot be met, the following wedge analysis can be used. The equations for the dynamic force given below for various conditions are simply the horizontal acceleration coefficient multiplied by the weight of the wedge defined by the critical slip-plane angle. See example 11 of Appendix M for sample calculations.

(1) Assumptions. The equations for determining the critical slip-plane angle for driving and resisting wedges subjected to a horizontal acceleration are developed with the following assumptions:

(a) The shear on the vertical face of the wedge is zero.

(b) The shear strength along the potential slip planes in the soil has not been mobilized to any extent, i.e., for static loading prior to an earthquake.

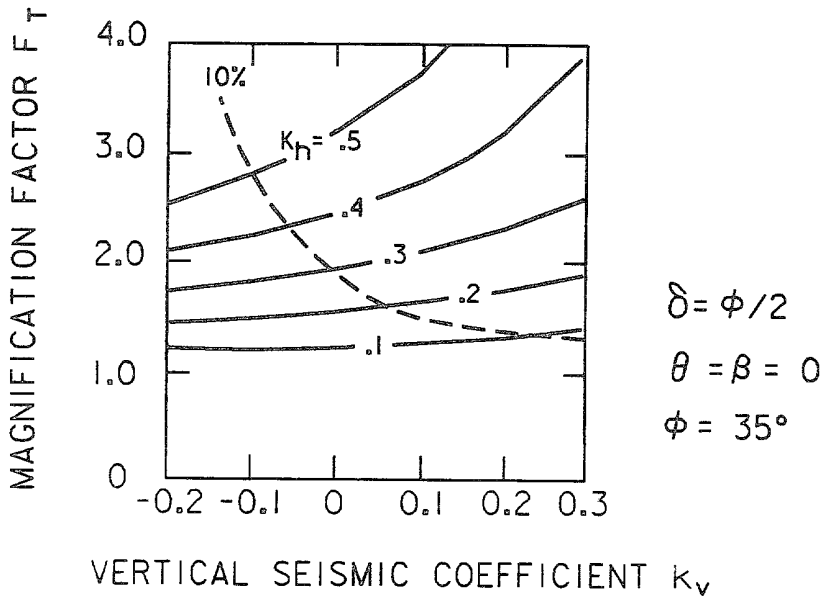

a. Influence of vertical seismic coefficient on magnification factor

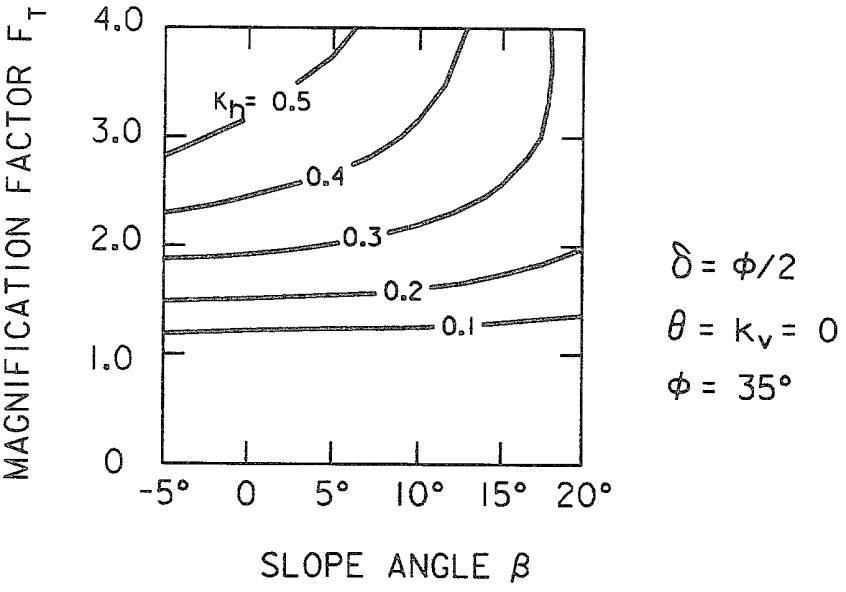

b. Influence of backfill slope angle on magnification factor

Figure 3-35. Influence of k_v and β on magnification factor (after Applied Technology Council 1981)

(2) Equations for Cohesionless, Dry Backfill Above the Water Table. Driving and resisting forces for cohesionless, dry, sloping planar-surfaced backfill below the water table where k_v, δ, and $\theta = 0$ can be computed as follows:

(a) Static Components. The static components for a driving and resisting wedge are:

$$P_A = \frac{1}{2} K_A \gamma h^2 \quad [3\text{-}52]$$

$$P_P = \frac{1}{2} K_P \gamma h^2 \quad [3\text{-}53]$$

where

$$K_A = \left(\frac{1 - \tan \phi \cot \alpha}{1 + \tan \phi \tan \alpha}\right)\left(\frac{\tan \alpha}{\tan \alpha - \tan \beta}\right) \quad [3\text{-}54]$$

$$K_P = \left(\frac{1 + \tan \phi \cot \alpha}{1 - \tan \phi \tan \alpha}\right)\left(\frac{\tan \alpha}{\tan \alpha - \tan \beta}\right) \quad [3\text{-}55]$$

as derived in paragraph H-2 and H-3, Appendix H.

For an active wedge:

$$\alpha = \tan^{-1}\left(\frac{c_1 + \sqrt{c_1^2 + 4c_2}}{2}\right) \quad [3\text{-}56]$$

$$c_1 = \frac{2 (\tan \phi - k_h)}{1 + k_h \tan \phi} \quad [3\text{-}57]$$

$$c_2 = \frac{\tan \phi (1 - \tan \phi \tan \beta) - (\tan \beta + k_h)}{\tan \phi (1 + k_h \tan \phi)} \quad [3\text{-}58]$$

For a passive wedge:

$$\alpha = \tan^{-1}\left(\frac{-c_1 + \sqrt{c_1^2 + 4c_2}}{2}\right) \qquad [3\text{-}59]$$

$$c_1 = \frac{2\,(\tan\phi - k_h)}{1 + k_h \tan\phi} \qquad [3\text{-}60]$$

$$c_2 = \frac{\tan\phi\,(1 + \tan\phi\tan\beta) + (\tan\beta - k_h)}{\tan\phi\,(1 + k_h \tan\phi)} \qquad [3\text{-}61]$$

If $k_v > 0$, replace γ with $(1 - k_v)\gamma$.

(b) Dynamic Components. The dynamic component for each wedge is:

$$\Delta P_{AE} = \Delta P_{PE} = k_h\left[\frac{\gamma h^2}{2\,(\tan\alpha - \tan\beta)}\right] \qquad [3\text{-}62]$$

(c) Total Driving Force. The total driving force is:

$$P_{AE} = P_A + \Delta P_{AE} \qquad [3\text{-}63]$$

which is equal to:

$$P_{AE} = \frac{1}{2} K_{AE}\gamma h^2 \qquad [3\text{-}64]$$

from the Mononobe-Okabe analysis.

The line of action for P_{AE} may be found as:

$$Y_{AE} = \frac{P_A\left(\frac{h}{3}\right) + \Delta P_{AE}\left(\frac{2h}{3}\right)}{P_{AE}} \qquad [3\text{-}65]$$

It should be noted that for large values of k_h , which cause α to be small,

P_A can be negative causing the line of action of P_{AE} to lie above the upper third point.

(d) Total Resisting Force. The total resisting force is:

$$P_{PE} = P_P - \Delta P_{PE} \qquad [3\text{-}66]$$

which is equal to:

$$P_{PE} = \frac{1}{2} K_{PE} \gamma h^2 \qquad [3\text{-}67]$$

from the Mononobe-Okabe analysis.

The line of action for P_{PE} may be found as:

$$Y_{PE} = \frac{P_P \left(\frac{h}{3}\right) - \Delta P_{PE} \left(\frac{2h}{3}\right)}{P_{PE}} \qquad [3\text{-}68]$$

(3) Equations for Cohesionless Backfill with Water Table. Driving and resisting forces for cohesionless, sloping, planar-surfaced backfill with water table where k_v, δ, and $\theta = 0$ can be computed as follows:

(a) Driving Force. The static components for a driving wedge are (see Figures 3-36a and 3-37a):

$$P_A = P_{A1} + P_{A2} = \frac{1}{2} K_A \gamma (h - h_s)^2 + \frac{1}{2} h_s \left[2K_A \gamma (h - h_s) + K_b \gamma_b h_s \right] \qquad [3\text{-}69]$$

$$P_{ws} = \frac{1}{2} \gamma_w h_s^2 \qquad [3\text{-}70]$$

and the dynamic components are (see Figures 3-36a and 3-37a):

$$\Delta P_{AE} = \Delta P_{AE1} + \Delta P_{AE2} = k_h \left[\frac{\gamma h^2}{2(\tan \alpha - \tan \beta)} \right] + k_h \left[\frac{(\gamma_s - \gamma) h_s^2}{2 \tan \alpha} \right] \qquad [3\text{-}71]$$

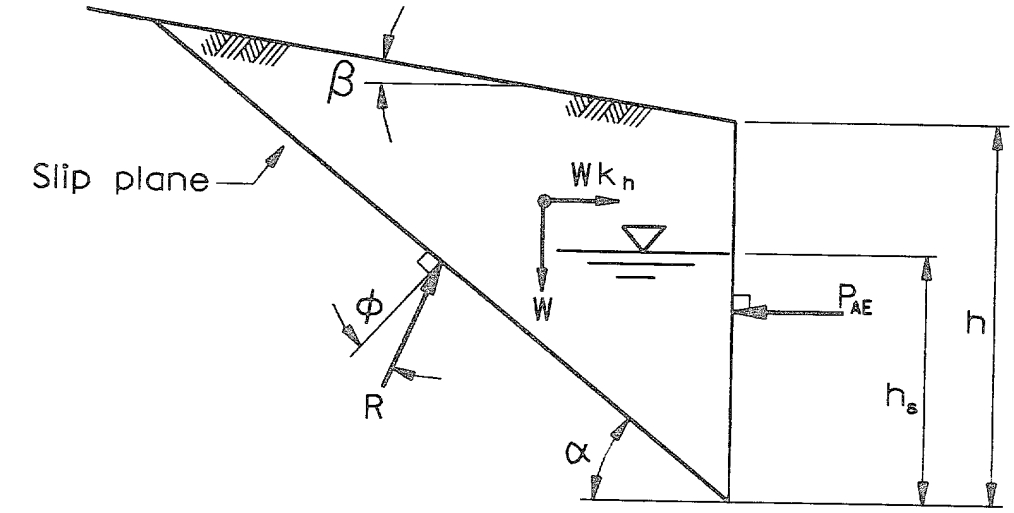

a. Driving wedge

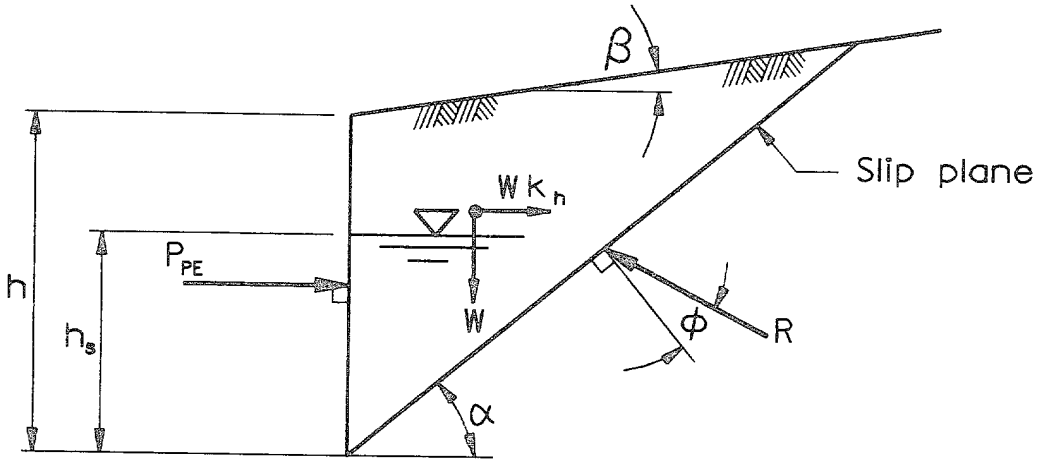

b. Resisting wedge

Figure 3-36. Seismic wedges, water table within wedge

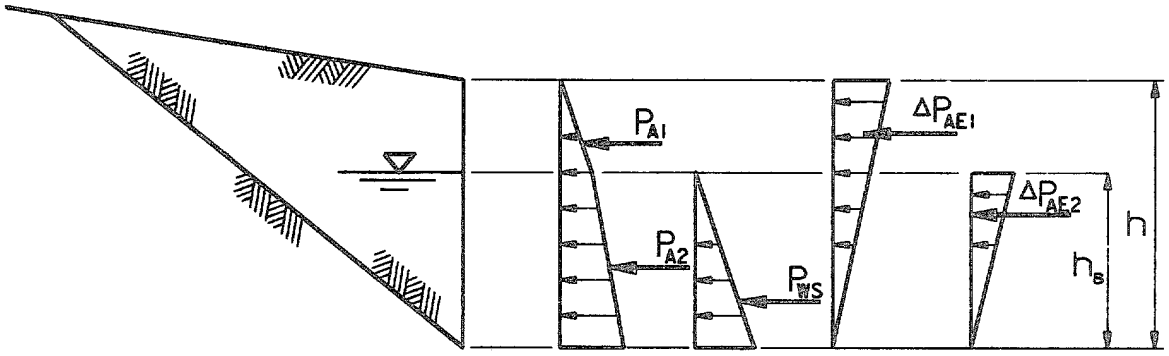

a. Driving wedge

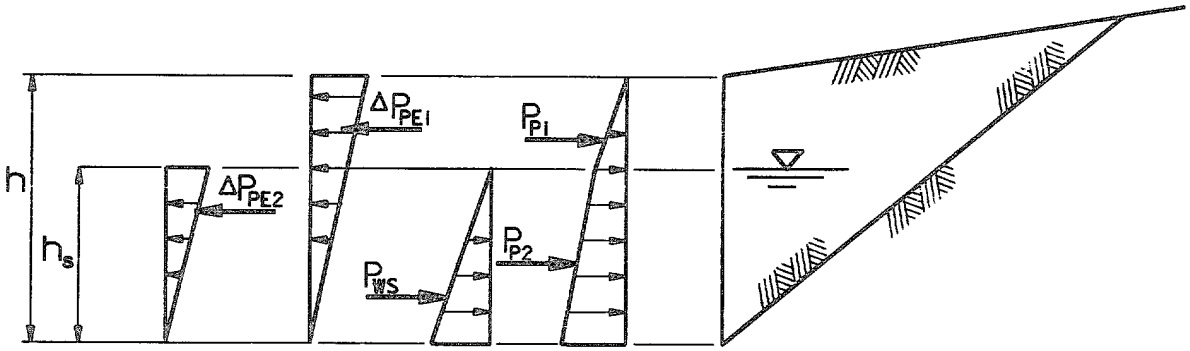

b. Resisting wedge

Figure 3-37. Static and dynamic pressure diagrams, water table within wedge

giving a total force of:

$$P_{AE} = P_A + P_{ws} + \Delta P_{AE} \qquad [3\text{-}72]$$

where

γ_s = saturated unit weight of fill

γ = moist unit weight of fill

γ_b = buoyant unit weight of fill

γ_w = unit weight of water

$$K_A = \left(\frac{1 - \tan \phi \cot \alpha}{1 + \tan \phi \tan \alpha}\right)\left(\frac{\tan \alpha}{\tan \alpha - \tan \beta}\right)$$

$$K_b = \left(\frac{1 - \tan \phi \cot \alpha}{1 + \tan \phi \tan \alpha}\right)\left[1 + \left(\frac{\tan \alpha}{\tan \alpha - \tan \beta} - 1\right)\frac{\gamma}{\gamma_b}\right]$$

and α is defined in Equation 3-56.

(b) Resisting Force. The static components for the resisting wedge are (see Figures 3-36b and 3-37b):

$$P_P = P_{P1} + P_{P2} = \frac{1}{2} K_P \gamma (h - h_s)^2 + \frac{1}{2} h_s \left[2K_P \gamma (h - h_s) + K_b \gamma_b h_s\right] \qquad [3\text{-}73]$$

$$P_{ws} = \frac{1}{2} \gamma_w h_s^2 \qquad [3\text{-}74]$$

and the dynamic components are:

$$\Delta P_{PE} = \Delta P_{PE1} + \Delta P_{PE2} = k_h \left[\frac{\gamma h^2}{2 (\tan \alpha - \tan \beta)}\right] + k_h \left[\frac{(\gamma_s - \gamma) h_s^2}{2 \tan \alpha}\right] \qquad [3\text{-}75]$$

giving a total force of:

$$P_{PE} = P_P + P_{ws} - \Delta P_{PE} \qquad [3\text{-}76]$$

where γ , γ_b , γ_s , and γ_w are defined in paragraph 3-26c(3)(a), and

$$K_P = \left(\frac{1 + \tan \phi \cot \alpha}{1 - \tan \phi \tan \alpha}\right)\left(\frac{\tan \alpha}{\tan \alpha - \tan \beta}\right) \quad [3\text{-}77]$$

$$K_b = \left(\frac{1 + \tan \phi \cot \alpha}{1 - \tan \phi \tan \alpha}\right)\left[1 + \frac{\tan \alpha}{\tan \alpha - \tan \beta} - 1\,\frac{\gamma}{\gamma_b}\right] \quad [3\text{-}78]$$

and the equations for α are given in Equation 3-59.

(4) Equations for Cohesive Backfill with Water Table. Driving and resisting forces for a cohesive, sloping, planar-surfaced backfill with water table where k_v , δ , and $\theta = 0$ can be computed as follows:

(a) Driving Force. The static components for the driving wedge are (see Figure 3-38a):

$$P_A = P_{A1} + P_{A2} = \frac{1}{2} K_A \gamma\left[(h - d_c) - h_s\right]^2 + \frac{1}{2} h_s\left[2K_A\gamma(h - d_c - h_s) + K_b\gamma_b h_s\right] \quad [7\text{-}79]$$

$$P_{ws} = \frac{1}{2} \gamma_w h_s^2 \quad [7\text{-}80]$$

and the dynamic components are (see Figure 3-38a):

$$\Delta P_{AE} = \Delta P_{AE1} + \Delta P_{AE2} = k_h\left[\frac{\gamma\left(h^2 - d_c^2\right)}{2\,(\tan \alpha - \tan \beta)}\right] + k_h\left[\frac{(\gamma_s - \gamma)^2 h_s^2}{2 \tan \alpha}\right] \quad [3\text{-}81]$$

giving a total force of:

$$P_{AE} = P_A + P_{ws} + \Delta P_{AE} \quad [3\text{-}82]$$

where

γ = moist unit weight of fill

γ_b = buoyant unit weight of fill

γ_s = saturated unit weight of fill

γ_w = unit weight of water

$$K_A = \left(\frac{1 - \tan\phi \cot\alpha}{1 + \tan\phi \tan\alpha}\right)\left(\frac{\tan\alpha}{\tan\alpha - \tan\beta}\right) \quad [3\text{-}83]$$

$$K_b = \left(\frac{1 - \tan\phi \cot\alpha}{1 + \tan\phi \tan\alpha}\right)\left[1 + \left(\frac{\tan\alpha}{\tan\alpha - \tan\beta} - 1\right)\frac{\gamma}{\gamma_b}\right] \quad [3\text{-}84]$$

$$\alpha = \tan^{-1}\left(\frac{c_1 + \sqrt{c_1^2 + 4c_2}}{2}\right) \quad [3\text{-}85]$$

$$c_1 = \frac{2\tan\phi\,(\tan\phi - k_h) + \frac{4c\,(\tan\phi + \tan\beta)}{\gamma(h + d_c)}}{A} \quad [3\text{-}86]$$

$$c_2 = \frac{\tan\phi(1 - \tan\phi\tan\beta) - (\tan\beta + k_h) + \frac{2c(1 - \tan\phi\tan\beta)}{\gamma(h + d_c)}}{A} \quad [3\text{-}87]$$

$$A = (1 + k_h \tan\phi)\tan\phi + \frac{2c(1 - \tan\phi\tan\beta)}{\gamma(h + d_c)} \quad [3\text{-}88]$$

$$d_c = \frac{c/\gamma}{\cos\alpha\,(\sin\alpha - \tan\phi\cos\alpha)} \quad [3\text{-}89]$$

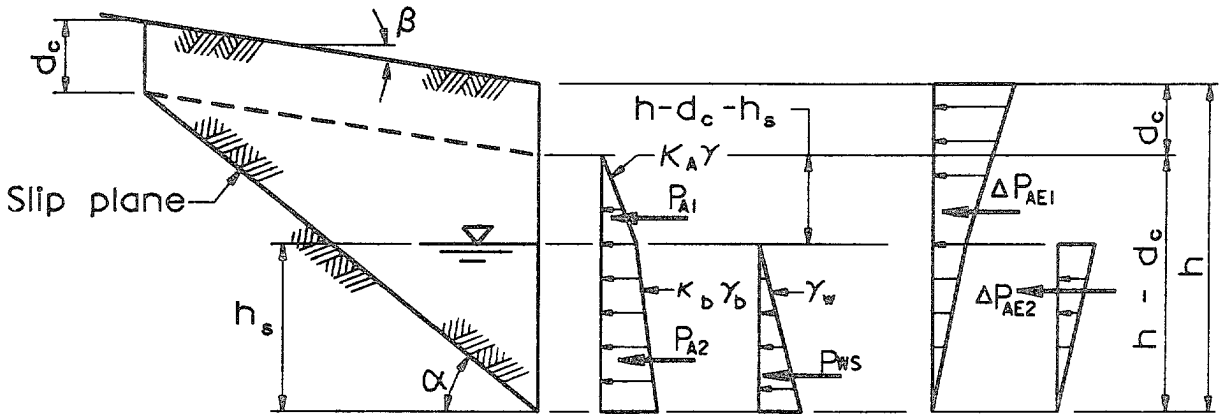

a. Driving wedge

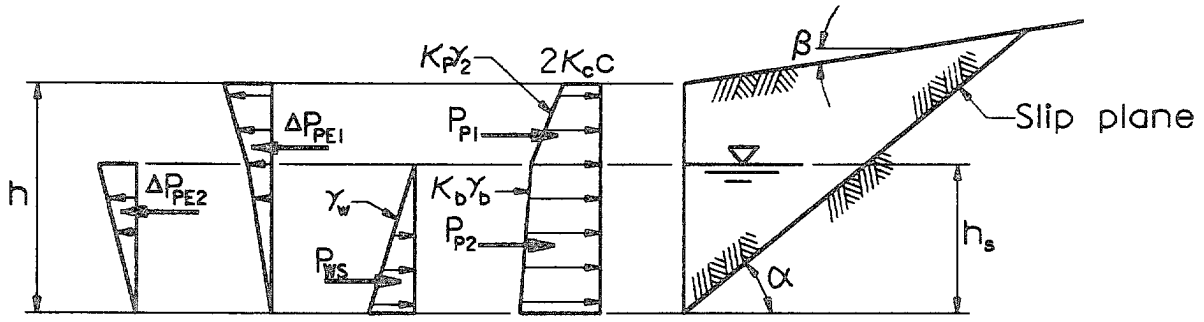

b. Resisting wedge

Figure 3-38. Static and dynamic pressure diagrams, cohesive fill, water table within wedge

(b) Resisting Force. The static components for the resisting wedge are (Figure 3-38b):

$$P_P = P_{P1} + P_{P2} = \frac{1}{2} K_P \gamma (h - h_s)^2 + \frac{1}{2} h_s \left[2K_P \gamma (h - h_s) + K_b \gamma_b h_s \right] + 2K_c ch \quad [3\text{-}90]$$

$$P_{ws} = \frac{1}{2} \gamma_w h_s^2 \quad [3\text{-}91]$$

and the dynamic components are (see Figure 3-38b):

$$\Delta P_{PE} = \Delta P_{PE1} + \Delta P_{PE2} = k_h \left[\frac{\gamma h^2}{2 (\tan \alpha - \tan \beta)} \right] + k_h \left[\frac{(\gamma_s - \gamma) h_s^2}{2 \tan \alpha} \right] \quad [3\text{-}92]$$

giving a total force of:

$$P_{PE} = P_P + P_{ws} + \Delta P_{PE} \quad [3\text{-}93]$$

where γ, γ_b, γ_s, and γ_w are defined in paragraph 3-26c(4)(a).

and

$$K_P = \left(\frac{1 + \tan \phi \cot \alpha}{1 - \tan \phi \tan \alpha} \right) \left(\frac{\tan \alpha}{\tan \alpha - \tan \beta} \right) \quad [3\text{-}94]$$

$$K_b = \left(\frac{1 + \tan \phi \cot \alpha}{1 - \tan \phi \tan \alpha} \right) \left[1 + \left(\frac{\tan \alpha}{\tan \alpha - \tan \beta} - 1 \right) \frac{\gamma}{\gamma_b} \right] \quad [3\text{-}95]$$

$$\alpha = \tan^{-1} \left(\frac{-c_1 + \sqrt{c_1^2 + 4c_2}}{2} \right) \quad [3\text{-}96]$$

$$c_1 = \frac{2 \tan \phi (\tan \phi - k_h) + \frac{4c (\tan \phi - \tan \beta)}{\gamma h}}{A} \quad [3\text{-}97]$$

$$c_2 = \frac{\tan \phi(1 + \tan \phi \tan \beta) + (\tan \beta - k_h) + \frac{2c(1 + \tan \phi \tan \beta)}{\gamma h}}{A} \quad [3\text{-}98]$$

$$A = (1 + k_h \tan \phi) \tan \phi + \frac{2c(1 + \tan \phi \tan \beta)}{\gamma h} \quad [3\text{-}99]$$

$$K_c = \frac{1}{2 \sin \alpha \cos \alpha (1 - \tan \phi \cos \alpha)} \cdot \frac{\tan \alpha}{\tan \alpha - \tan \beta} \quad [3\text{-}100]$$

d. Inertia Force of Wall. The inertia force of the wall, including that portion of the backfill above the heel or toe of the wall and any water within the backfill which is not included as part of the Coulomb wedge, is computed by multiplying the selected acceleration coefficient by the weight of the wall and backfill. This force is obtained by multiplying the mass by acceleration as follows:

$$F = ma = ma\left(\frac{g}{g}\right) = \frac{a}{g} w = k_h W \quad [3\text{-}101]$$

e. Hydrodynamic Force Due to Water Above Ground Level. Water standing above ground can have its static pressure, acting against a wall, increased or decreased due to seismic action. Figure 3-39 shows the pressures and forces due to earthquakes for freestanding water. The dynamic force is given by Westergaard's (1933) equation as:

$$P_E = \left(\frac{2}{3}\right) C_E k_h h^2 \quad [3\text{-}102]$$

where C_E is a factor depending upon the depth of water, h, in feet, and the earthquake period of vibration, T, in seconds. Westergaard's approximate equation for C_E in kip-second-foot units is:

$$C_E = \frac{0.051}{\sqrt{1 - 0.72\ (h/1000T)^2}} \quad [3\text{-}103]$$

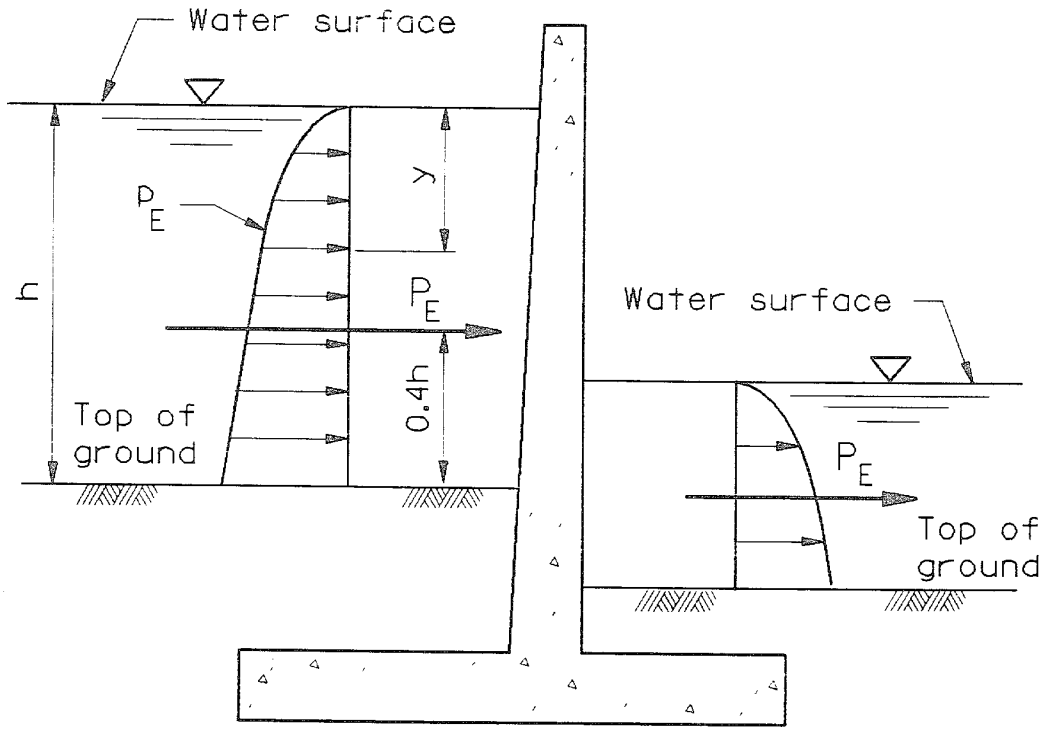

Figure 3-39. Hydrodynamic forces for freestanding water

Normally, for retaining and flood walls, C_E can be taken as 0.051. The pressure distribution is parabolic, and the pressure at any point y below the top surface is:

$$p_E = C_E k_h \sqrt{hy} \qquad [3\text{-}104]$$

The line of action of force P_E is 0.4h above the ground surface.

f. Selection of Acceleration Coefficients.

(1) Minimum Acceleration Coefficients. Minimum horizontal acceleration coefficient values for the United States and its Territories are listed in ER 1110-2-1806. In the absence of more accurate data, these values can be used as a guide for determining the acceleration coefficient to be used in the calculation of lateral earthquake forces on retaining and flood walls. As discussed in paragraph 3-26b(3)(d) where the horizontal ground acceleration is 0.2 g or less, the vertical ground acceleration can be neglected for all

practical purposes. When the vertical acceleration coefficient is included in the analysis, it is normally taken as two-thirds of the horizontal acceleration coefficient.

(2) Acceleration Coefficients Greater than 0.2. When the design acceleration coefficient exceeds 0.2, the Mononobe-Okabe analysis may require the size of the wall to be excessively great. To provide a more economical structure, design for a small tolerable lateral displacement rather than no lateral displacement may be preferable (Applied Technology Council 1981). A method for computing the magnitude of relative wall displacement during a given earthquake is described by Whitman and Liao (1985).

(3) Acceleration Coefficients for Walls Forming Part of a Dam. For retaining walls forming part of a dam, where failure of the wall would jeopardize the safety of the dam, the selection of the acceleration coefficients for the design of the wall should be consistent with those used for the stability analyses and concrete design of the dam, where required (ER 1110-2-1806).